# GRADUATE AERONAUTICAL LABORATORIES

# CALIFORNIA INSTITUTE OF TECHNOLOGY



## Turbulent free shear layer mixing and combustion

**Paul E. Dimotakis**

**GALCIT Report FM91-2**

**29 July 1991**



Firestone Flight Sciences Laboratory

Guggenheim Aeronautical Laboratory

Karman Laboratory of Fluid Mechanics and Jet Propulsion



Pasadena

# REPORT DOCUMENTATION PAGE

Form Approved
OMB No. 0704-0188



| 1. AGENCY USE ONLY (Leave blank) | 2. REPORT DATE | 3. REPORT TYPE AND DATES COVERED |
|---|---|---|
| | 29 July 1991 | GALCIT report |

**4. TITLE AND SUBTITLE**
Turbulent Free Shear Layer Mixing and Combustion

**5. FUNDING NUMBERS**
PE - 61102F
PR - 2308
TA - A2
G - AFOSR-90-0304

**6. AUTHOR(S)**
Paul E. Dimotakis

**7. PERFORMING ORGANIZATION NAME(S) AND ADDRESS(ES)**
Graduate Aeronautical Laboratories
California Institute of Technology
301-46
Pasadena, CA 91125

**8. PERFORMING ORGANIZATION REPORT NUMBER**
GALCIT report FM91-2

**9. SPONSORING/MONITORING AGENCY NAME(S) AND ADDRESS(ES)**
AFOSR/NA
Building 410
Bolling AFB DC 20332-6448

**10. SPONSORING/MONITORING AGENCY REPORT NUMBER**

**11. SUPPLEMENTARY NOTES**

**12a. DISTRIBUTION/AVAILABILITY STATEMENT**
Approved for public release; distribution is unlimited

**12b. DISTRIBUTION CODE**

**13. ABSTRACT (Maximum 200 words)**

Some experimental data on turbulent free-shear-layer growth, mixing, and chemical reactions are reviewed. The dependence of these phenomena on such fluid and flow parameters as Reynolds number, Schmidt number, and Mach number are discussed, with the aid of some direct consequences deducible from the large-scale organization of the flow as well as from some recent models.

| 14. SUBJECT TERMS | 15. NUMBER OF PAGES |
|---|---|
| | 68 |
| | 16. PRICE CODE |

| 17. SECURITY CLASSIFICATION OF REPORT | 18. SECURITY CLASSIFICATION OF THIS PAGE | 19. SECURITY CLASSIFICATION OF ABSTRACT | 20. LIMITATION OF ABSTRACT |
|---|---|---|---|
| Unclassified | Unclassified | Unclassified | UL |

GRADUATE AERONAUTICAL LABORATORIES
CALIFORNIA INSTITUTE of TECHNOLOGY
Pasadena, California 91125

# Turbulent free shear layer mixing and combustion*

Paul E. Dimotakis

## Abstract

Some experimental data on turbulent free-shear-layer growth, mixing, and chemical reactions are reviewed. The dependence of these phenomena on such fluid and flow parameters as Reynolds number, Schmidt number, and Mach number are discussed, with the aid of some direct consequences deducible from the large-scale organization of the flow as well as from some recent models.



GALCIT Report FM91-2

29 July 1991

---

* Earlier version presented at the 27th *AIAA Aerospace Sciences Meeting* (Reno, Nevada), 9–12 January 1989 (AIAA Paper 89-0262). Extended for the 9th ISABE (Athens, Greece), 3-9 September 1989. Revised and further extended with recent data, references, and additional discussions for publication as part of the *AIAA Progress in Astronautics and Aeronautics* volume on *Analysis of High Speed Propulsion Systems*

## 1. Introduction

The mixing of two or more fluids that are entrained into a turbulent region is an important process from both a scientific and an applications vantage point. Mixing in turbulent flows can imply a host of processes and phenomena. Species can be transported by turbulence to produce a more uniform distribution than some initial mean profile. This process is sometimes also referred to as mixing, without regard to whether the transported species are mixed on a molecular scale or not. If the issue of mixing arises in the context of chemical reactions and combustion, however, we recognize that only fluid mixed on a molecular scale can contribute to chemical product formation and associated heat release. The discussion in this paper will be limited to molecular mixing.

Molecular mixing by turbulence is important theoretically in that it provides an arena in which models of the behavior at the smallest scales of turbulence can be tested. These smallest scales correspond to a spectral regime that can be treated in a relatively cavalier fashion, if one need only address the *momentum* transport properties of the turbulent region (Brown and Roshko 1974), for example, but must be described with some deference to the physics at those scales if molecular mixing is to be accounted for correctly. From an experimental point of view, molecular mixing and chemical reactions in high-Reynolds-number flows provide us with an important probe of diffusion length and time scales that are so small as to otherwise remain beyond the reach of conceivable direct measurement diagnostics. Matters are no better computationally, with the requisite spatial/temporal resolution long recognized to be out of reach (e.g., Von Neumann 1949), a situation that must still be accepted as the case for high Reynolds number flow for the foreseeable future (e.g., Leonard 1983, Rogallo and Moin 1984). Finally, from a technological vantage point, mixing in a turbulent environment may well dictate the performance of many devices that rely on the details of the turbulent mixing process, such as high fuel efficiency internal combustion engines, chemical lasers, hypersonic propulsion, etc. It is also likely to prove to be an important consideration in other contexts, such the local and global environmental issues involving chemistry in the turbulent atmospheric environment, the dynamics of stellar atmospheres and interiors, etc.

The discussion here will be limited to mixing in turbulent shear layers, formed between two uniform free streams of unequal velocity, not necessarily of equal density, at high Reynolds numbers. In particular, at least for subsonic flow, for values of the local Reynolds number given by

$$Re \equiv \frac{\delta \Delta U}{\nu} > 10^4 , \qquad (1)$$

where $\delta = \delta(x)$ is the (local) transverse extent of the turbulent shear layer region,

$$\Delta U = U_1 - U_2 \tag{2}$$

is the velocity difference across the shear layer, and $\nu$ is some appropriate measure of the kinematic viscosity. In the discussion that follows, issues pertaining to gas-phase mixing will be addressed, for which the Schmidt number,

$$Sc \equiv \frac{\nu}{\mathcal{D}} , \tag{3}$$

with $\mathcal{D}$ the diffusing/mixing species diffusivity, is near unity. Mixing in liquid-phase flows, for which $Sc \gg 1$ (e.g., $Sc_{\mathbf{water}} \approx 600$), will also be discussed. Differences in turbulent mixing between these two fluid phases are important in that they provide important clues to the behavior and the dynamics of the flow at the smallest scales.

Although the two-dimensional, shear-layer flow geometry may not be germane to all the issues alluded to earlier, many of the phenomena that need to be addressed are generic and two-dimensional, turbulent, free-shear-layer flows provide a useful arena in which they can be studied. Additionally, however, the flow within the turbulent region formed between the two bounding free streams is capable of sustaining relatively rapid mixing, and one that can be further enhanced by a variety of flow manipulation means. This is a consequence of the property of shear-driven turbulence which, at least for subsonic flow conditions, can generate interfacial surface area between fluids inducted from each of the two streams at very high rates. At the high Reynolds numbers of interest here, the relatively small (molecular) diffusivity can result in a total diffusive flux across this very large interface that may come close to accommodating the rate at which the free stream fluids are inducted into the turbulent region at the largest scales of the flow. As a consequence, at least for subsonic, high-Reynolds-number, gas-phase flows, one finds that the expected fraction $\delta_{\mathrm{m}}/\delta$ of the turbulent region occupied by molecularly mixed fluid can be significant. It's not called a *mixing* layer for nought!

It is useful to view the molecular mixing process and any associated chemical product formation at a particular station $x$ of the flow as resolved into a sequence of Lagrangian stages in the "life" of entrained fluid elements bearing the chemical reactants. These fluid elements must:

1. be inducted into the mixing zone of relative transverse extent $\delta/x$, then,
2. mix molecularly to occupy some fraction $\delta_{\mathrm{m}}/\delta$, of $\delta(x)$ at $x$, before

3. reacting to form the chemical product, which represents, in turn, some fraction $\delta_P/\delta_m$ of the mixed fluid.

This suggests expressing the expected chemical product, formed between the virtual origin ($x = 0$) of the shear layer and the station at $x$, as a product of three factors, i.e.,

$$\frac{\delta_P}{x} = \frac{\delta}{x} \times \frac{\delta_m}{\delta} \times \frac{\delta_P}{\delta_m} . \tag{4}$$

The first factor, $\delta/x$, measures the *growth* of the mixing-layer region; the second, $\delta_m/\delta$, the *mixing* within the shear layer, and the third, $\delta_P/\delta_m$, the *chemical reactions* that can take place within the molecularly mixed fluid in the layer. This partition, at least in the case of high Reynolds numbers, is justified by the fact that the various stages represented by these factors occur in a *succession of Lagrangian times*. This resolution also provides a useful framework within which turbulent mixing and chemical reactions in two-dimensional shear layers can be discussed and reviewed and will be adopted in the discussion that follows.

## 2. Shear-layer growth: $\delta/x$

At the high Reynolds numbers of interest and for Schmidt numbers that, if not large, are not much smaller than unity, the shear-layer growth rate $\delta/x$ is an important quantity. It measures the angle of the wedge-shaped turbulent mixing region that confines the mixed fluid and chemical product. As a consequence, the width of the turbulent region, $\delta/x$, represents an upper bound for the amount of mixed fluid in the shear layer, corresponding to a scenario in which the entrained fluids are mixed instantly, on a molecular scale, as soon as they enter the turbulent region within the transverse extent $\delta$.

As we'll discuss below, the normalized transverse extent $\delta/x$ of the shear layer is found to depend on several dimensionless parameters of the flow, i.e.,

$$r \equiv \frac{U_2}{U_1} , \qquad s \equiv \frac{\rho_2}{\rho_1} , \tag{5}$$

the freestream velocity and density ratios, respectively, the (convective) Mach numbers of the two streams, i.e.,

$$M_{c1} = \frac{U_1 - U_c}{a_1} \qquad \text{and} \qquad M_{c2} = \frac{U_c - U_2}{a_2} , \tag{6a}$$

where

$$U_2 < U_c < U_1 \tag{6b}$$

is the convection velocity of the large-scale structures in the shear layer, and $a_{1,2}$ are the speeds of sound in the high- and low-speed freestream, respectively. In the case of combusting flow, it also depends on the relative mean density reduction $\Delta\rho/\rho$ in the interior of the chemically reacting shear layer attributable to heat release. For equal freestream densities ($\rho_1 = \rho_2 = \rho_0$), this can be expressed in terms of the heat release parameter

$$q \equiv \frac{\rho_0 - \bar{\rho}}{\rho_0} \equiv \frac{\Delta\rho}{\rho_0} , \tag{7}$$

where $\bar{\rho}$ is the (reduced) mean density of the flow within the $\delta/x$ shear-layer wedge. Finally, the shear layer growth rate is influenced by the presence of streamwise pressure gradients. We note, however, that if $dp/dx \neq 0$ (accelerating/decelerating flow), the shear layer will not grow linearly, unless it so happens that the dynamic pressures in the two free streams are matched, i.e., if $\rho_1 U_1^2 = \rho_2 U_2^2$ (Rebollo 1973). As we'll discuss later, experimental information, as well as some theoretical understanding, of the dependence of $\delta/x$ on these parameters is available, even though the picture is as yet far from complete or satisfactory.

By $\delta$, in this discussion, we will denote the local transverse extent of the sheared region that contains the molecularly mixed fluid in a boundary-layer sense, i.e., the distance between the shear layer edges outside which the expected concentration of molecularly mixed fluid is less than some small fraction, say, 1% of its peak value. This definition yields a local width that closely matches the measurements of the "visible" shear layer width $\delta_{\rm vis}$, as would be measured in a schlieren or shadowgraph picture of the layer (e.g., Brown and Roshko 1971, 1974). It is also very close to the 1% width, $\delta_1$, in the case of a chemically reacting layer, defined as the distance between the two points across the layer where the mean product concentration, or temperature rise owing to heat release, has dropped to 1% of its peak value (see Mungal and Dimotakis 1984, Koochesfahani and Dimotakis 1986). As a result of the similarity properties of this flow at high Reynolds numbers (Eq. 1), we can argue that other transverse scales must simply be proportional to the outer scale $\delta$. By way of example, the vorticity (or maximum slope) thickness $\delta_\omega$, defined in terms of the mean streamwise velocity profile $U(y)$ as

$$\frac{1}{\delta_\omega} \equiv \frac{1}{\Delta U}\left[\frac{{\rm d}U(y)}{{\rm d}y}\right]_{\rm max} , \tag{8}$$

is found to be roughly half of $\delta$.

## 2.1 Dependence on the velocity and density ratio

Abramowich (1963) and Sabin (1965) proposed an expression for the shear-layer growth rate given by

$$\frac{\delta}{x} \approx C_\delta \frac{1-r}{1+r} , \tag{9}$$

where $C_\delta$ is taken as a constant. This is an expression that can be argued for on similarity grounds,* and is found to be in reasonable accord with experimental data of incompressible shear layers with equal freestream densities. The dependence on the freestream density ratio was addressed in the seminal experiments by Brown and Roshko (1971, 1974), originally undertaken to investigate whether the observed reduction in growth rate in supersonic shear layers could be attributed to density ratio effects. Using different gases for each freestream and subsonic freestream

* In a frame moving with the convection velocity $U_c$, we must have $\delta/t \propto \Delta U$, where $\Delta U = U_1 - U_2$; the only relevant velocity in the problem. Equation 9 then follows if $U_c = (U_1+U_2)/2$, which is found to be the case for $\rho_1 = \rho_2$, if we transform back to the lab coordinates, i.e., $x = t/U_c$, and normalize all velocities with $U_1$.

velocities, they found that whereas the growth rate depended on the freestream density ratio, compressibility effects could not be identified with density ratio effects. In subsequent experiments, Konrad (1976) provided further documentation of the dependence on the density ratio and also noted that a shear layer entrained asymmetrically from each of the freestreams, as will be discussed in Sec. 3.2.

Brown (1974) proposed an account of these phenomena based on similarity arguments that recognized the significance of a Galilean frame translating at the convection velocity $U_c$ of the large structures. Growth and entrainment are to be understood as taking place in this frame, whose convection velocity is a function of both the density and velocity ratio. Brown's theory, which applied to a temporally growing shear layer, was in reasonable accord with the observed dependence of the growth rate on the freestream density ratio, but — as appropriate for a temporal model — predicted no asymmetry in the entrainment ratio for matched freestream densities, contrary to Konrad's observations.

In a subsequent proposal (Dimotakis 1984), the difference between temporal vs. spatial growth of a shear layer was noted and exploited to explain the entrainment ratio asymmetry. These basically geometric and similarity considerations led to an expression for the growth rate of a spatially growing shear layer given by

$$\frac{\delta}{x}(r,s;M\to 0) \;\approx\; C_\delta\,\frac{(1-r)(1+s^{1/2})}{2(1+s^{1/2}r)}\left\{1-\frac{(1-s^{1/2})/(1+s^{1/2})}{1+2.9(1+r)/(1-r)}\right\}\,, \qquad (10)$$

where the coefficient $C_\delta$ is taken as independent of the velocity ratio $r$ and the density ratio $s$. The factor multiplying the braces describes the growth rate of a temporally growing shear layer and is the same as the Brown proposal (1974) for shear layer growth. The factor in the braces arises from the fact that the growth is in fact spatial.

The observed (and predicted) dependence of the growth rate on the density ratio is not weak. It is plotted for density ratios in the range $0.1 < s < 8$ in Fig. 1, computed for a fixed velocity ratio of $r = 0.4$ and the value of $C_\delta = 0.37$, along with the experimental values of Brown and Roshko (1974) for $s = 1/7,\, 7$, and the measurement of Mungal and Dimotakis (1984) for $s = 1$. Also plotted for comparison is the Brown (1974) prediction for the temporally growing shear layer. As can be seen, the difference between the two predicted growth rates is not large. It vanishes for equal freestream densities ($s = 1$), where the quantity in the braces becomes equal to unity, and where the proposed expression reduces to the Abramowich-Sabin relation (Eq. 9).

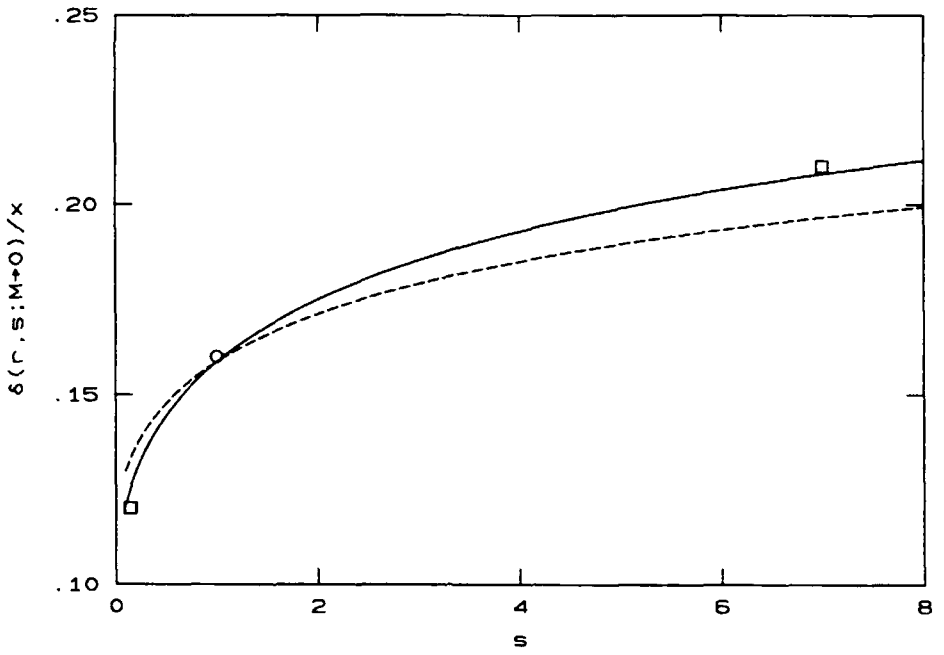


Fig. 1 Incompressible flow growth rate at fixed $r = U_2/U_1 = 0.4$ as a function of the density ratio $s = \rho_2/\rho_1$. Solid line: spatially growing layer (Eq. 10) with $C_\delta = 0.37$. Dashed line: temporally growing shear layer (Brown 1974). Squares: Brown and Roshko (1974), $s = 1/7, 7$. Circle: Mungal and Dimotakis (1984), $s = 1$.

For a free-shear layer with no external disturbances,** the value of the coefficient $C_\delta$ is found to be in the range of

$$0.25 \leq C_\delta \leq 0.45 \tag{11}$$

for the total thickness $\delta$, or roughly half that for the maximum slope thickness $\delta_\omega$ (cf. Eq. 8). See, for example, Brown and Roshko (1974, Fig. 10). An understanding, much less an accounting, of this rather large spread of values of the coefficient $C_\delta$, which cannot be attributed to experimental errors, must await further investigations. It is not even clear, at this writing, whether the inequality bounds in Eq. 11 represent actual limiting values, or not. What *is* clear is that this coefficient depends in some way on the initial conditions of the flow. See, for example, data and additional discussions in Batt 1975; Hussain 1978; Browand and Latigo 1979; Weisbrot, Einav, and Wygnanski 1982; Dziomba and Fiedler 1985; and Lang 1985.

** As opposed to a *forced*, or *driven*, shear layer (e.g., Oster and Wygnanski 1982, Husain and Hussain 1983, Ho and Huerre 1984, Roberts and Roshko 1985, Roberts 1985, Wygnanski and Petersen 1987, Koochesfahani and Dimotakis 1988).

It has been recognized for some time (Bradshaw 1966) that the shear layer is sensitive to its initial conditions. Bradshaw suggests that a minimum of several hundred of the initial momentum thicknesses $\theta_0$ is required for the shear layer to assume its asymptotic behavior. In view of the dynamics and interactions of the large-scale structures in the flow, it can even be argued that this estimate may not be conservative enough (Dimotakis and Brown 1976). These caveats notwithstanding, sufficient experimental data exist to suggest that a turbulent shear layer will exhibit *linear* growth, even within the Bradshaw $x/\theta_0$ specification, *but that the growth rate may not be a unique function of the freestream density and velocity ratio*. This is illustrated in the schlieren data in Fig. 2 of a shear layer with equal freestream densities ($s = 1$), as the flow velocity was increased, keeping the freestream velocity *ratio* fixed at $r = 0.4$. As can be seen, the reduction in the shear layer growth rate with increasing flow velocity is appreciable.

It is clear that this behavior cannot be attributed to effects scaled by the *local* Reynolds number, for example, which increases linearly with $x$ for this flow (see Eq. 1). Were that the case, or if *decaying* remnants of the effects of the initial conditions were responsible, the shear layer would be growing with curved edges rather than along (straight line) rays emanating from a virtual origin.

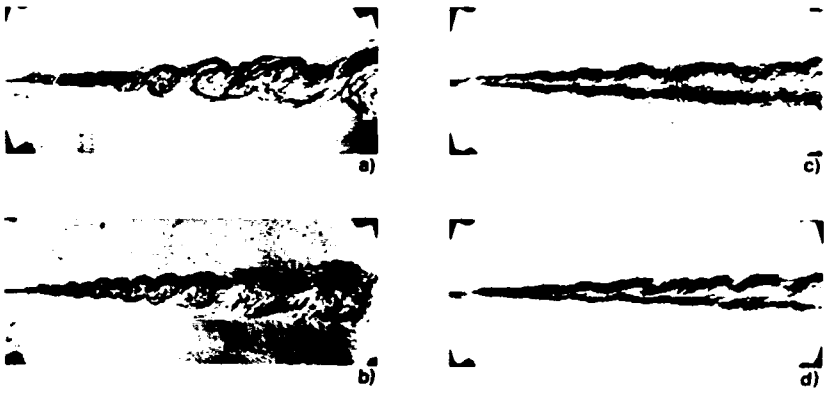


Fig. 2 Shear-layer growth at a fixed velocity ratio ($r = 0.4$) and equal freestream densities, as a function of flow velocity (field of view $\approx 25\,\mathrm{cm}$). The flow here is made visible by changes in the index of refraction owing to the (small) heat release from a diluted reactant $H_2 + F_2$ chemical reaction. (a) $U_1 = 13\,\mathrm{m/s}$, (b) $U_1 = 22\,\mathrm{m/s}$, (c) $U_1 = 44\,\mathrm{m/s}$, (d) $U_1 = 83\,\mathrm{m/s}$. Unpublished data by Mungal, Hermanson, and Dimotakis.

This behavior is perhaps better illustrated in the schlieren data in Fig. 3, formed as a composite of two pairs of pictures that cover roughly half a meter of

flow, corresponding to an $x/\theta_0$ of several thousand. The reader is invited to sight along the shear-layer edges of Fig. 3a, which is characterized by the better contrast, to ascertain the claim. Note that the highest high-speed stream velocity ($U_1$) in these data (Fig. 2) was 83 m/s, with the freestream fluid primarily composed of $N_2$ (diluent) gas. As a consequence, the observed reduction in growth rate cannot be attributed to compressibility (Mach number) effects, which will be discussed later.

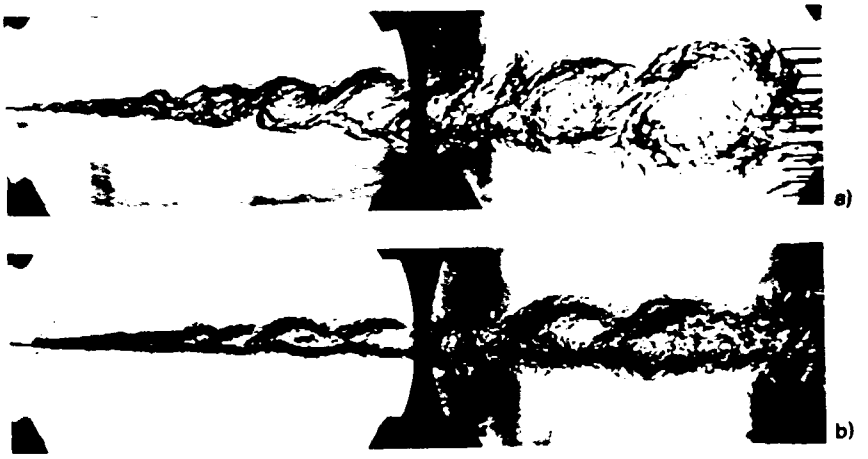


Fig. 3 Composite schlieren data of the same shear layer (probe array at far right at $x = 45$ cm). (a) $U_1 = 14$ m/s. (b) $U_1 = 88$ m/s. Unpublished data by Mungal, Hermanson, and Dimotakis.

It is intriguing that shear-layer growth, *as far downstream as several thousand of the original splitter-plate boundary-layer momentum thicknesses*, appears dependent on, if not determined by, the initial conditions. It is also intriguing that the large-scale structure spacing appears to be the same in the low- and high-speed flow data in Fig. 3, even as their transverse extent is being reduced: what does appear to be changing is the large-scale structure aspect ratio.

A clue to this behavior may, perhaps, be found in terms of the notions of *convective* and *global* instabilities, first developed in the context of plasma instabilities (Briggs 1964, Bers 1975). By that criterion and the results of temporal, linear stability analysis, the fluctuations in a (coflowing) plane shear layer must be classified as the former, as discussed in Huerre and Monkewitz (1985). In that context, it could be argued that the shear layer should be regarded as an amplifier of the externally imposed disturbances, possessing a nonunique growth rate thereby, as opposed to the behavior of an oscillator, which could be characterized by its own growth rate. In my opinion, however, that analysis is a (spatially) local analysis and must be

amended to include the contribution to the overall stability of the global effects of the initial development region, which is characterized by the influence of the wake introduced into the flow by the splitter plate (see, for example, discussion in Koch 1985) that Huerre and Monkewitz cite. See also Lang (1985), Koochesfahani and Frieler (1987), and Sandham and Reynolds (1987).

Finally, one would have to incorporate the additional feedback mechanisms present in the real flow in the analysis, such as the ones that act on the initial region owing to the long-range velocity fluctuations induced by the downstream structures, which span a range of *lower* frequencies, or pressure fluctuations feeding back to the splitter plate tip as the last structures leave the shear layer flow domain (test section), as dictated by the facility-dependent outflow boundary conditions (Dimotakis and Brown 1976). In addition to the long-coherence-time behavior of the autocorrelation functions discussed by Dimotakis and Brown, additional evidence in those experiments for this feedback was also available in the form of a flagellation of the initial region of the shear layer that was synchronous with the last exiting large-scale structure in the shear layer test section. Similar evidence was also gleaned from (unpublished) flow visualization data of the shear layer of Breidenthal (1981) that was generated in a rather different flow facility.

More recent, independent evidence of this feedback was obtained in our laboratory in the form of *upstream-propagating* (weak) normal shock waves in the low speed stream of a supersonic/subsonic shear layer (see Hall 1991, Figs. 4.16 and 4.17). While the mechanism that generates these waves is not completely clear, one can argue that they are likely to be caused by the oscillating-piston-like action of the fluctuating streamwise velocity component induced by the last exiting large-scale structure and its image on the lower flow guidewall — much like the mechanism operative in the low-speed shear layer visualizations discussed earlier. This feedback mechanism would, of course, be limited to subsonic flow, or, more precisely, to flow that connects the initial flow region and the downstream flow with an elliptical region. Its absence in purely supersonic flow deprives shear layer flows of an instability/amplification mechanism that is potentially important to the growth of the turbulent region.

A corollary of the existence of such long-range feedback mechanisms is that *local* descriptions of the dynamics of this flow may be inadequate. Certainly, the important differences between a *temporally* growing layer and the full scale, *spatially* growing shear layers of interest here must also be contended with. This difference was already noted in the context of the shear layer entrainment ratio. In the present

context, a local, temporal analysis also fails to represent the long-range coupling of the local behavior to non-local shear layer dynamics. The question of the applicability of *linear* stability analysis to the description of these phenomena aside, the classification of fluid mechanical instabilities into global and convective should also be assessed in this light; it derives from a local, temporal instability analysis. It is difficult to say, at this time, whether a proper accounting of all of these effects would alter the oscillator/amplifier qualitative classification of the behavior that stems from (temporal) convective/global instability analyses.

## 2.2 Compressibility effects

It has been documented that two-dimensional shear-layer growth decreases as the flow Mach number increases, even after the coupling of the flow Mach number to the freestream density and velocity ratio that would result in a typical flow facility is accounted for. See discussion in Brown and Roshko (1974, Sec. 7.1). Analysis (Bogdanoff 1983) and experimental investigations of compressible shear layers (Papamoschou and Roshko 1988) have suggested that, to a large extent, the effects of compressibility can be scaled by the *convective* Mach numbers of the shear-layer large-scale structures with respect to the two streams, which measure the relative freestream Mach numbers as seen from the Galilean frame of these structures (Eq. 6). It is interesting that one can also argue for a similar scaling on the basis of linear stability analysis of compressible shear flow, if the convection velocity $U_c$ is identified with the (real) phase velocity $c_r$ of the unstable mode in the flow (Mack 1975, Ragab and Wu 1988, Zhuang *et al.* 1988).

For incompressible flow, the convection velocity $U_c$ can be estimated by recognizing that, in the large-scale structure Galilean convection frame, stagnation points exist in between each adjacent pair of structures (Coles 1981). Continuity in the pressure at these points (Dimotakis 1984, Coles 1985), i.e.,

$$p_1 + \frac{1}{2}\rho_1 (U_1 - U_c)^2 \approx p_2 + \frac{1}{2}\rho_2 (U_c - U_2)^2 , \tag{12}$$

then yields, for $p_1 \approx p_2$,

$$\frac{U_1 - U_c}{U_c - U_2} \approx \sqrt{\frac{\rho_2}{\rho_1}} , \tag{13}$$

or,

$$\frac{U_c}{U_1} \approx \frac{1 + r\, s^{1/2}}{1 + s^{1/2}} . \tag{13'}$$

This agrees with the differently derived Brown (1974) result, the few estimates of this quantity from the $(x,t)$ data in Brown and Roshko (1974), as well as the measurements of Wang (1984) in curved shear layers. See also Coles (1985, Fig. 7) and related discussion.

For compressible flow, the corresponding result can be similarly estimated from the isentropic relation for the total pressure, i.e.,

$$\frac{p_{tj}}{p_j} = \left[1 + \frac{\gamma_j - 1}{2} M_{cj}^{(i)^2}\right]^{\frac{\gamma_j}{\gamma_j - 1}} , \tag{14a}$$

with $j = 1, 2$ corresponding to the high- and low-speed streams, $\gamma_j$ the ratios of specific heats, and $a_j$ the speeds of sound for the high-speed and low-speed stream fluids, respectively. The superscript '(i)' over the convective Mach number denotes that the estimate is based on isentropic pressure recovery assumptions.

Approximately equal pressure recovery from each freestream at the large structure interstitial stagnation points then yields (again, for $p_1 \approx p_2$)

$$\frac{p_{t1}}{p_1} \approx \frac{p_{t2}}{p_2} . \tag{14b}$$

This is the same result as the one arrived at by Bogdanoff (1983) using different arguments (see also discussion in Papamoschou and Roshko 1988). It also agrees with the linear stability estimates of this quantity (Zhuang *et al.* 1988), at least for subsonic convective Mach numbers. Note that, for equal ratios of specific heats ($\gamma_1 = \gamma_2$), e.g., if both freestreams are composed of monatomic gases, we have

$$M_{c1}^{(i)} \approx M_{c2}^{(i)} , \tag{15a}$$

or

$$r_c^{(i)} = \frac{U_1 - U_c^{(i)}}{U_c^{(i)} - U_2} \approx \frac{a_1}{a_2} , \tag{15b}$$

where, as above, the superscript '(i)' denotes an estimate based on isentropic pressure recovery assumptions. As can be seen, for static freestream temperatures that are also matched, the compressible, isentropic pressure recovery relation reverts to the incompressible, Bernoulli equation result (cf. Eq. 13).

It should be noted that these results are actually more robust than the assumption that the pressure recovered at the large-scale structure interstitial stagnation points can be computed assuming isentropic pressure recovery from each freestream. If only a *fraction* of the total pressure is recovered at these points, it suffices to assume that the losses from each side are roughly the same, in the mean. Considering the symmetries of the flow, even when viewed as an unsteady process, such an assumption may well be justified, at least for subsonic convective Mach numbers, and yields results in accord with the experimental data cited, as well as the computational evidence (e.g., Lele 1989) to date. Secondly, we should note that the pressure matching condition (Eqs. 12, 14) is not a *force* balance condition; the large-scale structure is not some intervening impermeable body between the two streams. If that were the case, a small "imbalance" that would momentarily decrease the velocity difference with respect to one stream would provide a *positive* feedback and drive the velocity difference with respect to the same stream to zero. This relation should rather be viewed as a nonlinear, quasistationary phase condition for the large-scale structures: any nonabiding flow substructure is subject to accelerations in its own frame, that will ultimately convect it with one or the other stream by the force of the positive feedback mechanism argument just cited. Perhaps the robustness of the large-scale flow structures in shear layers can be understood in this light. The positive feedback convection velocity mechanism strips away all other structures! The success of linear stability analyses of these phenomena, at least for subsonic convective Mach numbers, can perhaps also be understood in the same light, since the dominant surviving mode must abide by the same considerations.

Papamoschou and Roshko (1988) find that the compressible shear-layer growth rate, when normalized by the corresponding incompressible flow growth rate estimated at the same velocity and density ratio, is well represented as a function of the isentropically estimated convective Mach number only, say, $M_{c1}^{(i)}$, i.e.,

$$\frac{\frac{\delta}{x}\left[r, s; M_{c1}^{(i)}\right]}{\frac{\delta}{x}\left[r, s; M_{c1}^{(i)} = 0\right]} \approx \text{fn}\left[M_{c1}^{(i)}\right] \quad . \tag{16}$$

Figure 4 includes the data of Papamoschou and Roshko (1988), shear-layer growth-rate estimates computed from the earlier data of Chinzei *et al.* (1986) that were processed to estimate $M_{c1}^{(i)}$ for each of their runs and normalized to the value of $\delta(M_{c1}^{(i)})/\delta(0)$ at one point (filled circle), the data of Clemens and Mungal (1990), and the data of Hall *et al.* (1991). The smooth curve in Fig. 4 is a plot of the function

$$f(M_{c1}) = (1 - f_\infty)\, e^{-3M_{c1}^2} + f_\infty \quad . \tag{17}$$

It is drawn as a rough estimate of the effect, with a value for the asymptotic value of $f_\infty = 0.2$. See also Bogdanoff (1983) for an additional compilation of earlier data.

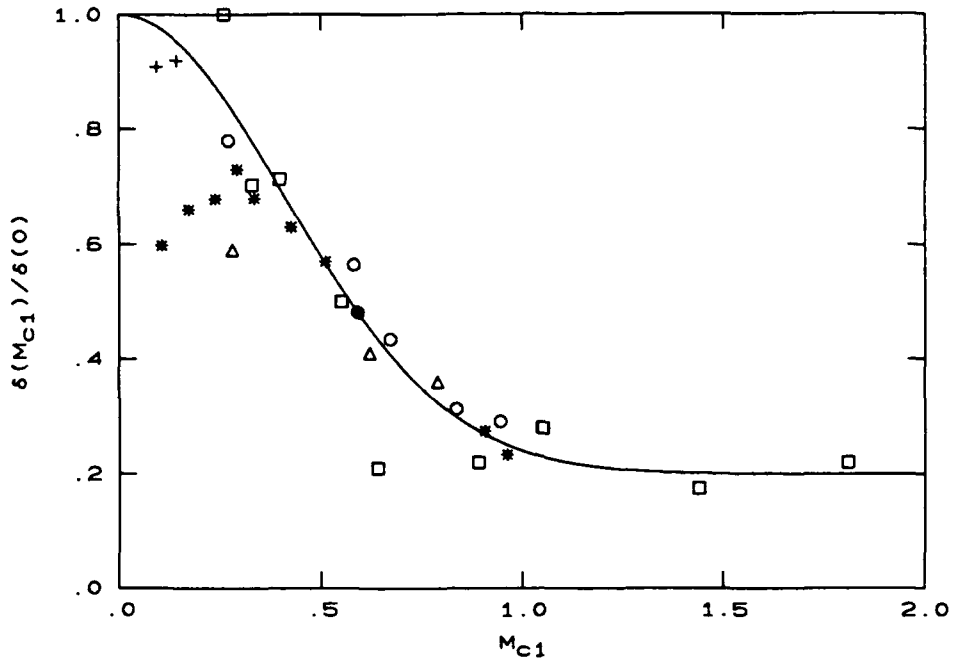


Fig. 4 Compressible shear-layer growth data, for a range of freestream velocity and density ratios, as a function of $M_{c1}^{(i)}$. Superscript '(i)' omitted from figure legend. Squares: Papamoschou and Roshko (1988) data. Circles: growth rates estimated from the Chinzei *et al.* (1986) data, normalized to the filled point. Triangles: data of Clemens and Mungal (1990). Stars: $M_1 > 1$ data of Hall *et al.* (1991a). Crosses: $M_1 < 1$ data of Hall *et al.* (1991a). Smooth curve is a plot of Eq. 17.

The data in Fig. 4 suggest that the convective Mach number need not be very large for compressibility effects to be significant. Secondly, for $M_{c1}^{(i)} > 0.8$, the growth rate appears to reach an asymptotic value roughly 0.2 of its incompressible counterpart. This is at variance with the results of two-dimensional, linear, shear-layer stability analyses (e.g., Gropengiesser 1970, Ragab and Wu 1988, Zhuang *et al.* 1988), which find that the growth rate tends to very small values, as $M_{c1}^{(i)} \rightarrow \infty$. If the stability analysis results are accepted at face value, the applicability of such an analysis aside for the moment, the discrepancy could be attributable to other factors. In particular, it appears likely that three-dimensional modes are more unstable in the limit of large Mach numbers, as was suggested by Sandham and Reynolds (1989a). Alternatively, the Papamoschou and Roshko experiments were conducted in an enclosed test section, as opposed to the stability analyses which

were carried out for unbounded flow. For supersonic convective Mach numbers, a closed test section can act as a wave guide, providing a feedback mechanism between the growing shear layer structures and the compression/expansion wave system whose energy would otherwise be radiated and lost to the far field (Tam and Morris 1980, Tam and Hu 1988, Zhuang *et al.* 1990). Finally, recalling our aside, we should recognize that, for supersonic (or even transonic) convective Mach numbers, we expect shocks to form in the flow, a feature that cannot adequately be captured by *linear* stability analysis.

It should be noted that it is not clear at this writing whether the observed limiting value of the ratio $\delta[M_{c1}^{(i)}]/\delta[M_{c1}^{(i)}=0]$, for $M_{c1}^{(i)} \gg 1$, is intrinsic to the behavior of the fully developed compressible shear layer, or depends on the details of the flow geometry, e.g., the distance of the upper and lower flow guide walls from the layer, whether only one or both streams are supersonic, etc. In the context of the potential for hypersonic air-breathing propulsion and flight, for example, whether the growth rate tends to zero with increasing Mach number is an important issue; an ever decreasing shear layer growth with increasing Mach number hardly bodes well for efficient supersonic mixing and combustion!

As can be seen in the data in Fig. 4, there are some "rogue" points at low convective Mach numbers, from the data of Hall *et al.* (1991a). It is significant that all the supersonic shear layer flow data of Hall *et al.* were taken at the same high-speed freestream Mach number of $M_1 \simeq 1.5$. For these shear layers, the various values of the convective Mach number were realized using different compositions for the freestream gases. The low growth rates of the "rogue" points corresponded to shear layers with low freestream density ratios, i.e., for $\rho_2/\rho_1 \ll 1$. On the basis of these data, we may infer that the utility of the convective Mach number as the scaling parameter of compressibility effects on shear-layer growth rates, which is based on a temporal growth picture in the Galilean frame moving with the turbulent structures, cannot describe all the factors that influence this behavior. Additional evidence of this shortcoming will be discussed later.

Subsequent to his initial investigations, Papamoschou (1989) conducted a series of experiments in which he investigated the convection velocity of the large-scale structures, for a range of freestream Mach numbers and various gases. In those experiments, he found that, at high convective Mach numbers, the large-scale structures seemed to be "dragged" by one stream or another, at variance with the matched, isentropic pressure recovery model of Eq. 14. See Fig. 5a for a plot of the

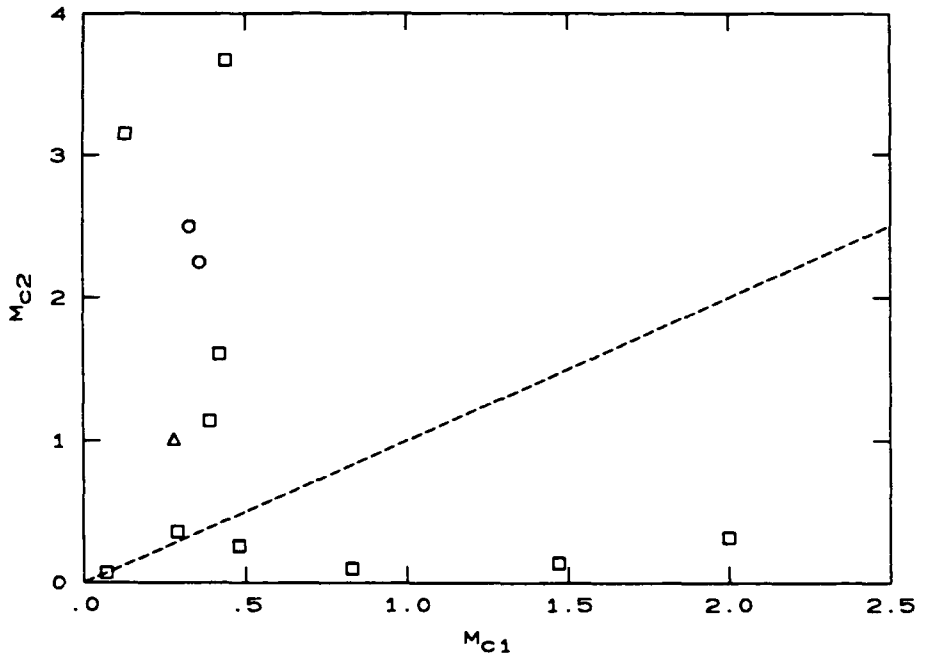


Fig. 5a Supersonic shear layer ($M_1 > 1$) convective Mach number experimental data of Papamoschou (1989, squares); Fourguette *et al.* (1990, triangle) and Hall *et al.* (1991a, circles). Dashed line computed for $\gamma_1 = \gamma_2$, assuming $U_c = U_c^{(i)}$ (Eq. 15a).

Papamoschou (1989) and some additional, more recent, data.† As can be seen, the experimental data are found to be close to the isentropically estimated values only for convective Mach numbers less than 0.5, or so. Papamoschou (1988, 1989) offered a qualitative description of how shocks could be responsible for this behavior, crediting D. Coles for the suggestion, which was made before the experiments were conducted, that the effects of shocks needed to be incorporated in the analysis.

We can appreciate that for supersonic, or transonic, convective Mach numbers the freestream flow over the turbulent large-scale structures can support a system of expansions and shocks. As a consequence, the assumption of isentropic, approximately matched, pressure recovery from each stream (Eq. 14) can be expected to be inadequate at supersonic convective Mach numbers. In that case, streamlines that end up on interstitial stagnation points from each freestream will have to traverse a shock, or, more likely, a system of shocks for turbulent flow, to connect to the freestream static conditions and will have suffered a loss in total pressure that may be reasonably well approximated by that of a normal shock.

† The point $(M_{c1}, M_{c2})$ derived from the Fourguette *et al.* (1990) data was computed using the quoted (directly measured) value for the convection velocity of $U_c = 352\,\mathrm{m/s}$.

This leads to the following possibilities, depending on which stream has, or can support, shocks. In particular, we can have shocks in the high-speed stream, with a shock-free low-speed stream, i.e.,

$$\frac{p_{s1}}{p_1} \approx \frac{p_{t2}}{p_2} \; ; \tag{18a}$$

low-speed stream shocks, with a shock-free high-speed stream, i.e.,

$$\frac{p_{t1}}{p_1} \approx \frac{p_{s2}}{p_2} \tag{18b}$$

while for shocks in both streams, we must have

$$\frac{p_{s1}}{p_1} \approx \frac{p_{s2}}{p_2} \; . \tag{18c}$$

In these expressions, $p_t/p$ is the isentropic total-to-static recovery pressure ratio (Eq. 14) and $p_s/p$ is the ratio of the post-normal shock total pressure to the free stream static pressure, given by (Rayleigh pitot tube formula),

$$\frac{p_s}{p} = \left( \frac{\gamma+1}{2} M_s^2 \right)^{\gamma/(\gamma-1)} \left( \frac{2\gamma}{\gamma+1} M_s^2 - \frac{\gamma-1}{\gamma+1} \right)^{-1/(\gamma-1)} \tag{19}$$

for $M_s > 1$, where $M_s$ is the shock Mach number (e.g., Liepmann and Roshko 1957, p. 149).

As was noted by Papamoschou (1989), the estimation of the convective velocity $U_c$ of the turbulent structures using these relations requires the shock Mach number $M_s$ to be specified, which is not known a priori. This issue was addressed in a recent proposal (Dimotakis 1991), which is briefly outlined below.

Returning to Fig. 5a, for convective Mach numbers that are not small, we see that the data appear to fall in two groups: decidedly above, or below, the $M_{c1} = M_{c2}$ dashed line (cf. Eq. 15 and related discussion). These two groups correspond to supersonic shear layers with subsonic and supersonic low-speed streams, respectively. In the context of the previous discussion, we can understand this by assuming that, for $M_1 > 1$ and $M_2 < 1$, the shocks are borne by the low-speed freestream, whereas, for purely supersonic flow, i.e., $M_1, M_2 > 1$, the shocks are borne by the high speed stream. We will accept this as an empirical *stream selection rule*.

For subsonic, but near sonic, convective Mach numbers, evidence for the formation of shocks can be found in the calculations of Lele (1989), and Vandromme and Haminh (1989, cf. Fig. 2), for example, where one expects weak shocks (dubbed "shocklets") confined to the vicinity of the shear zone. See cartoon in Fig. 6a. No experimental evidence for these transonic shocklets is available at this writing.

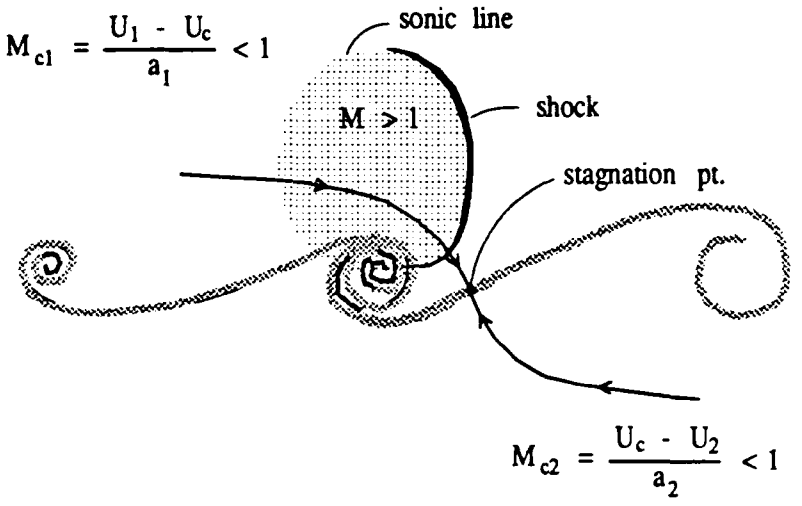


Fig. 6a Proposed vortex/shock configuration cartoon, sketched for a shock borne by the high speed stream and a transonic convective Mach number, i.e., $M_{c1} < 1$.

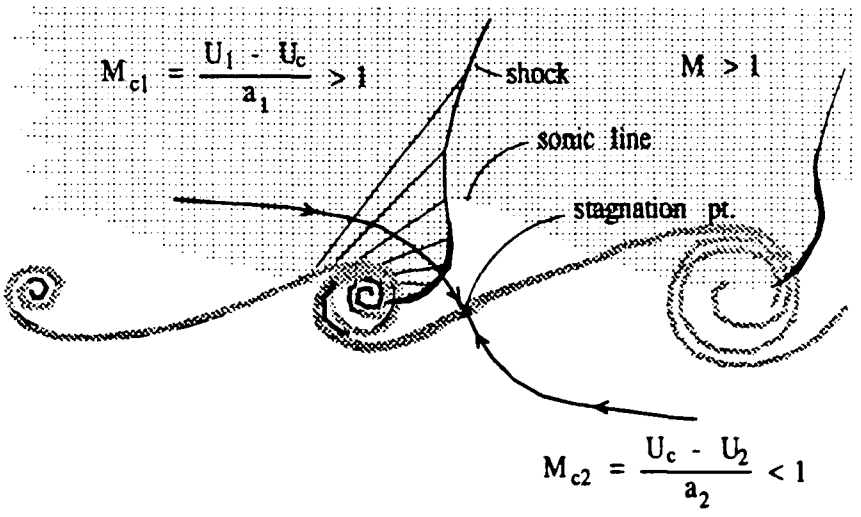


Fig. 6b Proposed supersonic vortex/shock configuration cartoon, sketched for a supersonic convective Mach number ($M_{c1} > 1$).

For supersonic convective Mach numbers, experimental evidence has been available for turbulent-structure-generated shocks from the core region of supersonic jets, i.e., Lowson and Ollerhead (1968), Tam (1971), and Oertel (1979). More recently, such evidence has been documented in our laboratory for a two-dimensional,

supersonic shear layer in Hall *et al.* (1991a) and Hall (1991). In the Hall *et al.* experiments, a shock/expansion wave system extending into one of the free streams, as sketched in Fig. 6b, was found.

An example of such a wave system, for a $M_1 = 1.5$ He high speed stream, over $M_2 = 0.35$ Ar low speed stream shear layer, is reproduced in Fig. 7 (from Hall *et al.* 1991a, Fig. 5). See also Hall (1991, Fig. 4.11) for similar data from a $M_1 = 1.5$ He high speed stream, over $M_2 = 0.3$ $N_2$ low speed stream shear layer.

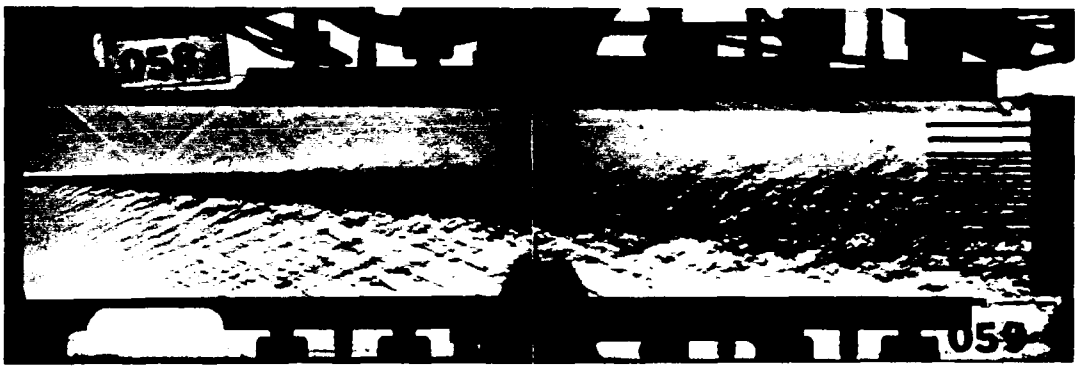

Fig. 7 Schlieren data for a $M_1 = 1.5$ He high speed stream, over $M_2 = 0.35$ Ar low speed stream shear layer. Note travelling oblique shock system in low speed stream (Hall *et al.* 1991a, Fig. 5).

Given the freestream $j$ that carries the shocks and the shock Mach number, $M_{sj}$, or, equivalently, a given shock strength parameter

$$X_j \equiv \frac{M_{sj}}{M_{cj}} \ , \tag{20}$$

the convection velocity can be estimated by computing the total pressure loss through the shocks (cf. Eqs. 18). This yields a continuum of solutions for $U_c$ vs. the shock strength parameter $X_j$.

With these assumptions, the strength of the shock can be estimated if the turning angle $\Delta\theta$ through which the flow has been expanded, prior to crossing the near-normal shock, is known. The turning angle $\Delta\theta_j$ in the $j^{\text{th}}$ stream can be estimated, in turn, as the difference of the corresponding Prandtl-Meyer angles between the flow just ahead of the shock and the free stream (or sonic conditions), i.e.,

$$\Delta\theta_j \ = \ \theta_{\text{PM}}(M_{sj}) - \theta_{\text{PM}}(M_{cj}) \ , \qquad \text{for} \qquad M_{cj} \ \geq \ 1 \ , \tag{21a}$$

where $\theta_{PM}(M)$, defined for $M > 1$, is the Prandtl-Meyer angle function (e.g., Liepmann and Roshko 1957, p. 99). If the convective Mach number $M_{cj}$ in the $j^{th}$ stream is close to, but less than, unity (transonic $M_{cj}$), the turning angle $\Delta\theta_j$ will be computed using

$$\Delta\theta_j = \theta_{PM}(M_{sj}) , \qquad \text{for} \qquad M_{cj} < 1 . \tag{21b}$$

The latter is equivalent to starting the calculation at the location where the streamline crosses the sonic line to enter the supersonic bubble. See cartoon in Fig. 6a.

Depending on the flow parameters, the pressure-matching condition can lead to several solution branches. Given the free stream that carries the shock and the shock strength, several branches will typically exist, with a continuum of solutions for the convection velocity $U_c$ as a function of the shock strength parameter $X$. The proposed ansatz is that *the convection velocity of the large scale structures is such as to render the flow stationary*. One can argue for this conjecture by noting that if the shock-generating flow structures are to represent a quasi-steady, convecting flow configuration, they must be able to persist in the presence of turbulent fluctuation disturbances.

We note here that a Galilean-invariant analysis, i.e., one based on the temporal behavior of the large scale structures in the convected frame, as in the cartoons in Figs. 6a and 6b, *cannot* capture the (laboratory frame) empirical stream selection rule for the stream that carries the shocks cited above. As a consequence, we will accept the value derived from the proposed stationary flow ansatz when it yields solutions in accord with the empirical selection rule.

When the flow is computed as a function of the shock strength parameter $X_j = M_{sj}/M_{cj}$, corresponding to a shock in the $j^{th}$ stream, one finds that the solution branches fall into two classes. In the first solution class, Type I flow, the turning angle $\Delta\theta$ can be computed by assuming that the flow chooses the stream $j$ and the shock Mach number, i.e., the shock strength parameter $X_j = M_{sj}/M_{cj}$, so as to render the turning angle $\Delta\theta_j$ stationary (a maximum). This corresponds to a stable flow configuration wherein small changes in the shock Mach number $M_{sj}$ result in quadratically small changes in $\Delta\theta_j$. Alternatively, in Type II solutions, it is the shock strength parameter $X_j$ that is stationary with respect to small changes in the turning angle $\Delta\theta$, corresponding to the maximum admissible value for $X_j$ that yields a solution for $U_c$.

It is found that both Type I and Type II solutions can be admissible (in the same flow). In the latter case, one can argue for a selection rule which favors the Type I branch, over the Type II solution branch, as being the more robust configuration of the two. If more than one solution branch of the same type is possible, the proposed selection rule is that the branch that yields the *lower* total pressure is chosen by the flow. In other words, the flow will try to satisfy the pressure matching condition at the lowest stagnation pressure possible, generating the shock with the requisite strength. See Dimotakis (1991) for a more detailed discussion.

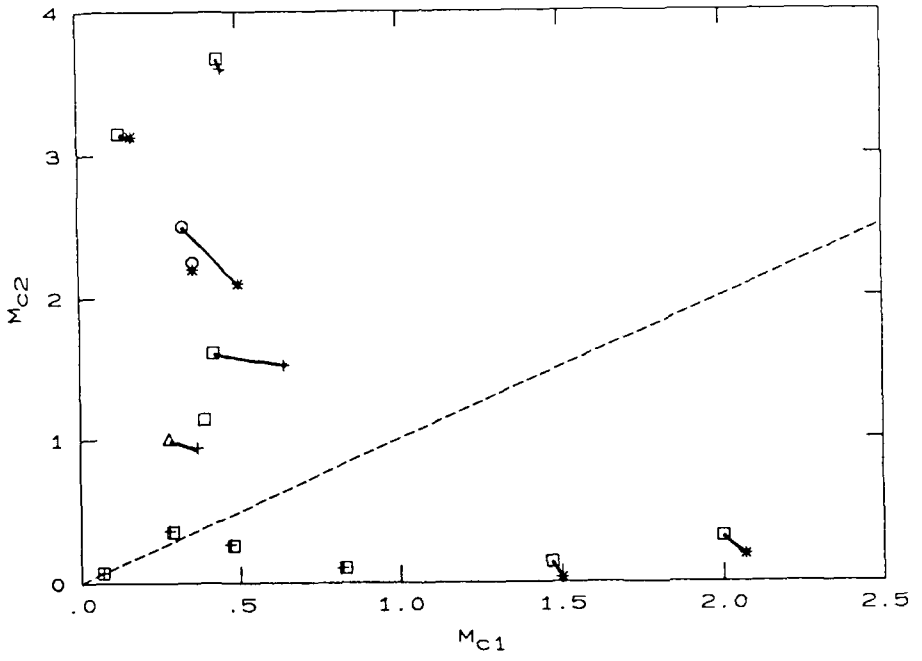


Fig. 5b Experimental data of $(M_{c1}, M_{c2})$ from Fig. 5a. Computed points are joined to corresponding flow data points by straight lines, asterisks corresponding to Type I and crosses corresponding to Type II flows.

The results of calculations based on the proposed scheme are summarized in Fig. 5b, which compares the experimental data in Fig. 5a with the theoretical calculations. The estimates, based on the proposed scheme, for flows found to yield Type I solutions are denoted by asterisks, while those corresponding to Type II solutions are denoted by crosses. If the computed values are found to fall outside the extent of the experimental data point symbols, they are joined to the corresponding data points by straight lines. There is one case for which the stationary shock is borne by the stream that is not accord with the empirical stream selection rule.

This corresponds to the $M_1 = 3.2\,\mathrm{Ar}$ and $M_2 = 0.2\,\mathrm{Ar}$ shear layer of Papamoschou (1989). No computed $(M_{c1}, M_{c2})$ point is indicated for it.

It may be interesting to also ask for input from linear stability analyses of this flow, with the appreciation that finite amplitude wave effects, such as the loss in total pressure associated with entropy production in shock waves, cannot properly be captured by such analyses. Nevertheless, the very small entropy generation from weak oblique shocks, as would be expected under many flow conditions, might render linear stability analysis results useful for convective Mach numbers that are not too high. Such an investigation was specifically undertaken by Sandham and Reynolds (1989b). The agreement for low convective Mach numbers is quite good. At higher convective Mach numbers, however, the linear stability analysis calculations underestimate the departure of the convection velocity from the isentropically computed values. As was noted, this is as one would anticipate. It is interesting that stability analysis appears to predict the correct shock-bearing stream for the case not computed in Fig. 5b, but predicts the wrong one for the flow with the highest $M_{c2}$. See Sandham and Reynolds (1989b, Fig. 2.25).

We may conclude that available data to date appear to be reasonably well accounted for by assuming the existence of a turbulent structure, convecting with a well-defined speed and generating a set of shocks in one of the two free streams. There is some evidence, however, that shear layers at higher flow Mach numbers yet the shear layer may support shocks in both streams (Oertel 1979). If that is borne out by future experiments, we can expect that the large asymmetries in the apparent velocity ratio $r_c$ in the turbulence convection frame, i.e.,

$$r_c \equiv \frac{U_1 - U_c}{U_c - U_2} \,, \tag{22}$$

documented in Fig. 5, will be mitigated by the more symmetric flow configuration of turbulent-structure-generated shocks borne by both freestreams.

These results are important in a variety of contexts. From the point of view of chemical reactions and combustion, the apparent velocity ratio $r_c$ (Eq. 22) seen by the turbulent structures is an important factor in the shear layer entrainment ratio and the consequent stoichiometric composition of the molecularly mixed fluid in the layer, as we will discuss later. The stream selection rule and the proposed ansatz of shock strengths selected by the condition of stationarity suggest that one can expect jumps in $r_c$, potentially, as a result of small changes in the flow parameters.

From a theoretical vantage point, we should recall that the empirical stream selection rule is not Galilean-invariant and, therefore, it cannot be captured by the type of analysis outlined above. As was noted in the context of the discussion on shear layer growth rate, the fact that a supersonic/subsonic shear layer contains an elliptical region connecting the inflow and outflow boundary conditions needs to be incorporated in the analysis. Evidence of the need for a global, rather than local, description of these flows was also discussed earlier in the context of the use of the convective Mach number to account for the compressibility effects on shear-layer growth rates. At least for shear-layer flows which include an elliptical region, i.e., a subsonic low-speed freestream, it would appear that a more complicated description is required. The resolution of these and other issues must await the results of several investigations currently in progress.

## 2.3 Heat-release effects

Some experimental investigations have studied the effects of heat release on the growth rate of chemically reacting shear layers (e.g., Wallace 1981, Hermanson and Dimotakis 1989), as well as experiments with combusting shear layers at high levels of heat release (e.g., Ganji and Sawyer 1980, Pitz and Daily 1983, Daily and Lundquist 1984, Keller and Daily 1985). Useful information has also been derived from computations (e.g., McMurtry *et al.* 1986, McMurtry and Riley 1987), which is in qualitative accord with the experimental findings, even though these computations have perforce been conducted at Reynolds numbers that do not meet the fully developed flow criterion of Eq. 1.

One might argue that dilatation owing to heat release in a chemically reacting shear layer, which is confined to the shear-layer wedge, might result in an *increase* in shear-layer growth. Although the basis of that intuition is well founded, the inference is not. One does observe a *displacement* velocity in the far field away from the shear layer, which increases with the amount of heat released. This can be measured experimentally as a displacement thickness $\delta^*/x$ by noting the angle of, say, the lower freestream flow guide wall required to maintain a nonaccelerating flow ($\mathrm{d}p/\mathrm{d}x = 0$), as a function of the amount of heat release. See Fig. 8.

At least for subsonic flow and equal freestream densities, other parameters held constant, one observes a *decrease* in the shear-layer growth rate with increasing heat release. This behavior is depicted in the data of the 1% thickness in Fig. 9, taken

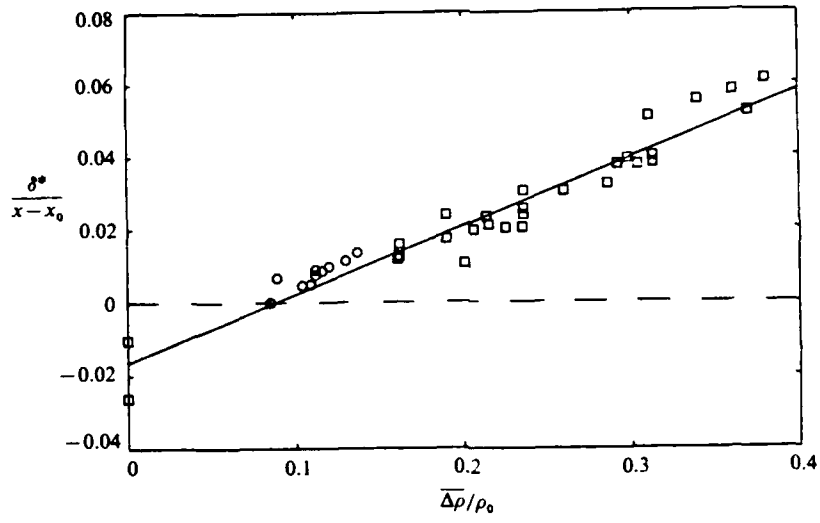


Fig. 8 Normalized shear-layer displacement thickness vs. heat release. Circles: Mungal (unpublished) data. Squares: Hermanson and Dimotakis (1989).

from Hermanson and Dimotakis (1989, Fig. 5). Note that, in these experiments, the pressure gradient was maintained close to zero by adjusting the lower stream guide wall as necessary. These data suggest that the decrease in the shear-layer growth rate with heat release is approximately given by ($q = \Delta\rho/\rho$, recall Eq. 7)

$$\frac{\frac{\delta}{x}(r = 0.4,\, s = 1;\, q)}{\frac{\delta}{x}(r = 0.4,\, s = 1;\, q = 0)} \approx 1 - C_q\, q \;, \tag{23a}$$

with

$$C_q \approx 0.05 \;. \tag{23b}$$

While these experiments were conducted at a fixed velocity ratio $r = 0.4$ and matched freestream densities ($s = 1$), one can speculate that heat-release effects manifest themselves as a reduction in the growth-rate coefficient $C_\delta$ (Eqs. 9 and 10), with Eq. 23 expressing the dependence of $C_\delta$ on $q$. In any event, at least for subsonic shear layers, the effect of heat release on the growth rate is slight (see also Daily and Lundquist 1984).

The physical implication is that the outward displacement velocity owing to heat release impedes the entrainment process to an extent that more than offsets the effects of dilatation. It is interesting that this reduction in growth rate is also found to be consistent with the assumption that the heat release and dilatation effects leave the $\overline{u'v'}$ velocity correlation largely unaltered. The reduction in the growth rate can then be approximately accounted for by noting the reduction in

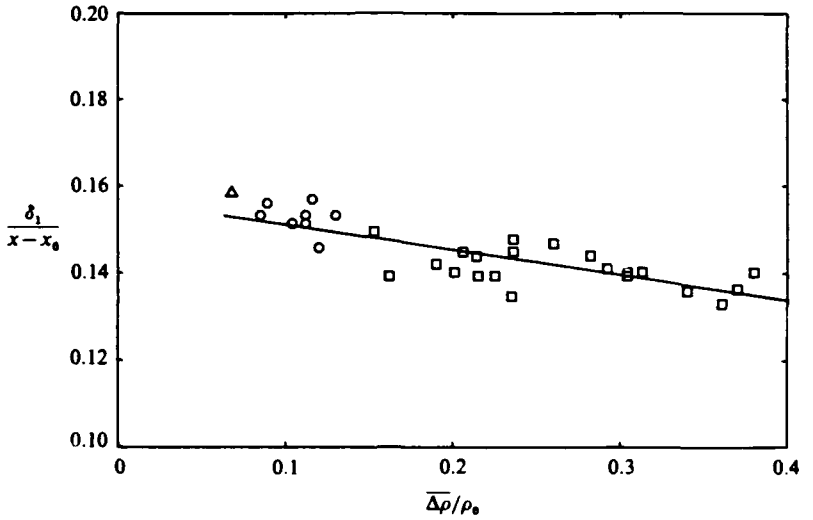


Fig. 9 Normalized 1% thickness vs. heat release. Triangle: Wallace (1981). Circles: Mungal (unpublished data). Squares: Hermanson and Dimotakis (1989). Note displaced origin.

the turbulent stress $\tau = \overline{\rho u' v'}$ in the layer; a result of the reduction in the density profile $\rho\,(y/x)$ owing to heat release. It should be noted that it would probably be difficult to argue for such an assumption a priori. See discussion in Hermanson and Dimotakis (1989), Secs. 5.2 and 5.4.

At high Reynolds numbers, a substantial volume fraction in the turbulent shear layer is occupied by fluid that is *not* molecularly mixed (independently estimated to be roughly 1/2 at the conditions of the Hermanson and Dimotakis experiments) so that, even with fast chemical reactions characterized by large adiabatic flame temperatures, there will be a limiting value of the expected reduction in $\Delta\rho/\rho$ within the layer owing to heat release. This is a consequence of the large pockets of entrained, unmixed fluid whose density is essentially unaltered by the combustion process. This behavior is illustrated by the data in Fig. 10, where the estimated mean density reduction $\Delta\rho/\rho_0$ is plotted vs. the normalized adiabatic temperature rise $\Delta T_f/T_0$. These data were recorded at high Reynolds numbers ($Re \approx 6 \times 10^4$), for several values of the freestream stoichiometric mixture ratio $\phi$, an important quantity that we will discuss later in the context of chemical reactions.

A useful test model of the behavior with increasing heat release is one in which vortical structures tend to a configuration of low-density (hot) cores and are surrounded by irrotational, recently entrained, unmixed (cold) fluid. Using this picture, the expected mean density reduction in the combustion zone can be estimated. In

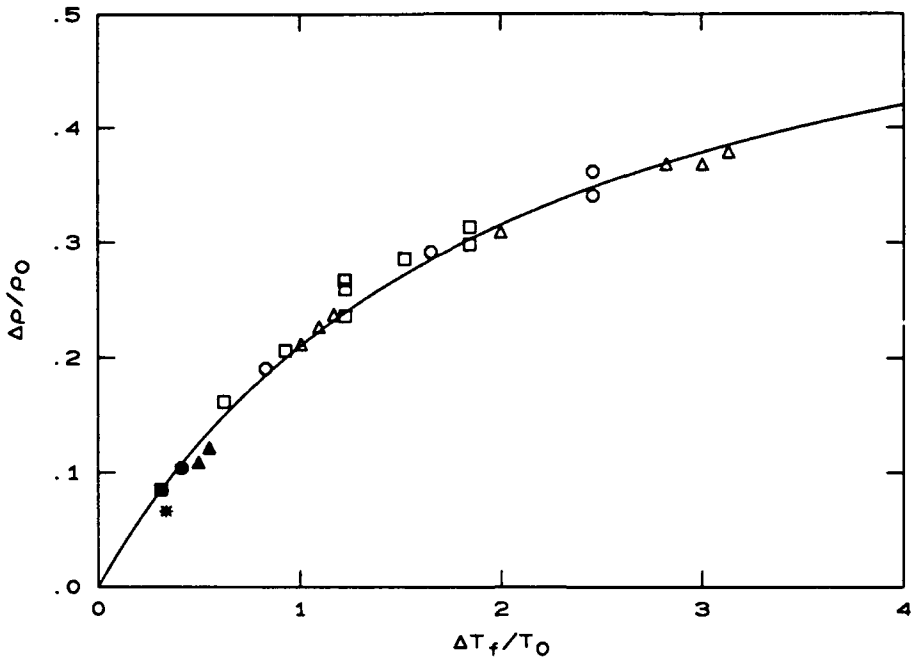


Fig. 10 Mean density reduction $\Delta\rho/\rho$ vs. adiabatic flame temperature rise $\Delta T_f/T_0$, where $T_0$ is the (common) freestream temperature. Squares/asterisk: $\phi = 1$. Circles: $\phi = 1/2$. Triangles: $\phi = 1/4$. Solid symbols: Mungal and Dimotakis (1984). Open symbols: Hermanson and Dimotakis (1989). Asterisk: Wallace (1981). Smooth line computed using Eq. 23.

the notation of Eq. 4, we find

$$\frac{\Delta\rho}{\rho_0} \approx \frac{\left(\frac{\delta_P}{\delta}\right)\frac{\Delta T_f}{T_0}}{1 + \left(\frac{\delta_P}{\delta_m}\right)\frac{\Delta T_f}{T_0}} \ . \tag{23a}$$

The smooth line in Fig. 10 was computed using this expression and constant, heat-release-independent values of

$$\frac{\delta_m}{\delta} = 0.63 \ , \qquad \frac{\delta_P}{\delta_m} = 0.5 \ . \tag{23b}$$

It is interesting that the resulting curve does as well as it does, suggesting that the simple model may have merit even at moderately high values of the heat release. As we shall see later, the inferred value of 0.63 of the mixed fluid fraction $\delta_m/\delta$ is a little high. It should be noted, however, that the mean density reduction values in Fig. 10 were estimated here using the reciprocal of the mean temperature measured in the combustion zone, as opposed to the mean of the reciprocal temperature, which would have provided better estimates. Additionally, of course, the mixed fluid fraction is not likely to be exactly constant, i.e., independent of $\Delta T_f/T_0$.

## 2.4 Pressure gradient effects

The effects of pressure gradient on shear layer growth were discussed by Sabin (1965) and have been investigated in non-reacting shear layers (Rebollo 1973), and in reacting shear layers (Keller and Daily 1985, Hermanson and Dimotakis 1989) for incompressible flow conditions. In the case of a favorable pressure gradient ($\mathrm{d}p/\mathrm{d}x < 0$) and equal free stream densities ($s = \rho_2/\rho_1 = 1$), it was found (Hermanson and Dimotakis 1989) that the decrease in the growth could be accounted by interpreting Eq. 9 as a local relation. The argument, which was suggested by M. Koochesfahani and is akin to some of the ideas put forth by Sabin (1965), is summarized below.

The local rendition of the Abramowich-Sabin relation (Eq. 9) becomes

$$\frac{\mathrm{d}\delta}{\mathrm{d}x} \approx C_\delta \frac{1 - r(x)}{1 + r(x)} , \tag{24a}$$

with

$$r(x) \equiv \frac{U_2(x)}{U_1(x)} \tag{24b}$$

the local velocity ratio. This can be computed by applying the Bernoulli equation in each of the freestreams, and yields

$$r(x) = r_0 \sqrt{\frac{1 - C_{p2}(x)}{1 - s\, r_0^2\, C_{p2}(x)}} , \tag{25a}$$

where

$$r_0 \equiv \frac{U_2(0)}{U_1(0)} \tag{25b}$$

is the freestream velocity ratio at $x = 0$,

$$C_{p2}(x) \equiv \frac{p(x) - p(0)}{\frac{1}{2}\rho_2 U_2^2(0)} \tag{25c}$$

is the local pressure coefficient normalized by the low-speed stream dynamic head at $x = 0$, and $s = \rho_2/\rho_1$ is the freestream density ratio. It can be seen that a favorable pressure gradient is expected to decrease, or increase, the shear-layer growth rate, depending on whether the product $s\, r_0^2$ is less, or greater than, unity, respectively. The converse is true for an unfavorable pressure gradient.

For a specified pressure gradient, Eq. 25 for the local velocity ratio can be used to integrate the local growth rate (Eq. 24) to yield the local shear layer width $\delta\,[C_{p2}(x)]$ at the station $x$. The results of this procedure are in accord with the observed effects, at least for the range of values of the pressure coefficient at the measuring station that were investigated (Hermanson and Dimotakis 1989, Sec. 8).

## 3. Mixing: $\delta_m/\delta$

As alluded to in the preceding discussions, one finds that, at sufficiently high Reynolds numbers, a substantial fraction of the fluid within the $\delta/x$ shear-layer wedge is not molecularly mixed. Additionally, at least for incompressible shear layers, the available evidence suggests that the mixed fluid in a turbulent shear layer exhibits the following characteristics:

1. The mixed fluid composition (averaged across the shear-layer width $\delta/x$) is *not* generally centered around a 50:50 mixture but favors a composition that is a function of the freestream density and velocity ratio.
2. The amount of mixed fluid, beyond the downstream location where the shear layer has attained fully developed, three-dimensional flow status (e.g., Eq. 1), depends weakly on the local flow Reynolds number. The evidence suggests that, at least for gas-phase shear lavers, it decreases as the Reynolds number increases.
3. The mixed fluid fraction $\delta_m/\delta$ is found to depend on the fluid Schmidt number $Sc \equiv \nu/\mathcal{D}$ (Eq. 3).

A large number of models are employed today in efforts to account for the observed turbulent shear-layer mixing phenomena and, whereas they all differ in the details of their implementation, they can be classified, in my opinion, into two main categories: models that ultimately rely on some form of Reynolds averaging and/or turbulent gradient transport, and models that do not. In the discussion that follows, models which cannot account for the characteristics just listed will not be considered in the attempt to account for shear-layer mixing phenomena. Although it could be argued that this need not be so, this criterion, to the best of my knowledge, presently eliminates models that rely on gradient transport ideas. For an opposing viewpoint, the reader is directed to the review article by Bilger (1989) and references therein. Unfortunately, since molecular mixing takes place throughout the spectrum of spatial and temporal scales, direct computations at high Reynolds numbers are out of the question for now, at least, and we must resort to some kind of modeling for some time.

It may appear surprising that *Schmidt* number effects are given so much weight when it could be argued that most turbulent mixing/combustion phenomena are encountered in gas-phase flows. There are two issues here. First, although it may be

that *most* turbulent combustion occurs in gas phase flows, it is certainly not so that *all* of it does (cf. underwater, liquid metal, particulate combustion, etc.). Second, if we are to formulate models on which we must rely for predictions and design outside the range of experience that was used to validate them, and not just use them as interpolative french curves, we must at least require that they adequately account for the *known* turbulent mixing behavior. In the case of Schmidt number effects, the issue is particularly important, inasmuch as those effects are a direct manifestation of, and provide important clues to, the role of the small mixing scales of the problem, which must be correctly accounted for (if not described) by turbulent mixing models.

## 3.1 The mixing transition

The flow in a two-dimensional shear layer issuing from a smooth splitter plate with a sharp trailing edge and low-turbulence-level freestreams originally develops as two-dimensional flow. This flow is characterized by large, two-dimensional, vortical structures (e.g., Winant and Browand 1974, Corcos and Sherman 1984), but is susceptible to a three-dimensional instability mode of counter-rotating streamwise vortices (Konrad 1976, Bernal 1981, Alvarez and Martinez-val 1984, Corcos and Lin 1984, Daily and Lundquist 1984, Browand 1986, Bernal and Roshko 1986, Metcalfe *et al.* 1987, Knio and Ghoniem 1988, Lasheras and Choi 1988, Rogers and Moser 1991), which spawn the transition to three-dimensional, fully developed turbulent flow, leading to substantial increases in the mixed fluid fraction (Konrad 1976, Bernal *et al.* 1979, Breidenthal 1981, Roberts 1985, Koochesfahani and Dimotakis 1986). This is illustrated in the liquid-phase flow laser-induced fluorescence data reproduced in Fig. 11, recorded before ($Re \approx 2 \times 10^3$) and after ($Re \approx 2.3 \times 10^4$) the mixing transition, respectively. Note that, in the pre-mixing-transition data, the entrained fluids participate in the large-scale motion but remain essentially unmixed. Under these conditions, the surface-to-volume ratio of the two-dimensional interfacial area between the two entrained fluids is relatively small. In particular, when multiplied in water ($\mathcal{D} \approx \nu/10^3$) with the small local transverse diffusion thickness straddling this interface, i.e.,

$$\lambda_{\mathcal{D}} \propto \sqrt{\mathcal{D}/\sigma} \ , \tag{26}$$

where $\sigma$ is the (local) strain rate (see Marble and Broadwell 1977, Broadwell and Breidenthal 1982, and Dimotakis 1987, Sec. 2.2), it yields a negligible mixed fluid volume fraction $\delta_{\rm m}/\delta$ within the shear layer width $\delta/x$.

Fig. 11 Liquid-phase shear-layer mixing digital $(y,t)$ image data at a fixed streamwise location $x$ (Koochesfahani and Dimotakis 1986). Left image: pre-mixing-transition ($Re \approx 2 \times 10^3$). Right image: post-mixing-transition ($Re \approx 2.3 \times 10^4$).

The large increase in interfacial area following the mixing transition changes this tally, resulting in a mixed fluid fraction, under these conditions, of

$$\delta_m/\delta \approx \begin{cases} 0.26\,, & \text{in water;} \\ \\ 0.49\,, & \text{in gas-phase flow.} \end{cases} \tag{27}$$

We will substantiate these values later. It is interesting that the growth rate of the shear layer does not appear to respond to this mixing transition, suggesting that it is dominated by the two-dimensional large-scale dynamics (see Fig. 3 and also discussion in Corcos and Lin 1984). The evolution of $\delta(x)$ and $\delta_m(x)$ through the mixing transition is sketched in Fig. 12.

It is not clear, at this time, how this picture is altered by compressibility effects, or even whether the criterion of a minimum local Reynolds number of $10^4$ will be good when the convective Mach numbers become large. The depressed growth rate of the two-dimensional Kelvin-Helmholtz disturbances, discussed in the previous section, may well alter the environment in which the three-dimensional motions develop, which are vital for the large interfacial area generation (see also Demetriades 1980; Demetriades, Ortwerth and Mooney 1981; and Demetriades and Brower 1982). At higher convective Mach numbers, shocks can certainly be expected to play an important role in this process. Whether that role enhances a transition to three-dimensionality and improved mixing must also await future investigations.

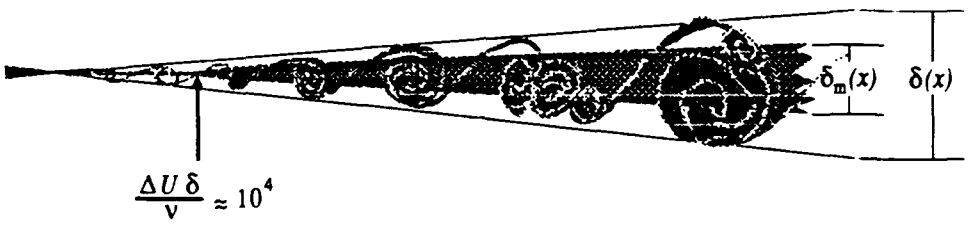


Fig. 12 Sketch of shear layer and gas-phase mixed fluid thickness growth through the mixing transition.

### 3.2 Entrainment ratio

We can think of the growth of the shear-layer region $\delta/x$ as the increasing participation of freestream fluid in the turbulent process, i.e., the *entrainment*, as the downstream distance from the splitter plate increases. In this context, the preceding discussion on shear-layer growth addresses the *total* entrainment flux from each of the two freestreams, without regard as to the relative amounts from each freestream, i.e., the entrainment flux *ratio*. It is clear, however, that the entrainment flux ratio, that is supplied to the mixing processes of turbulence, must be taken into account in the tally of the resulting range of compositions of the mixed fluid.

An important conclusion drawn by Konrad (1976) was that *a shear layer entrains fluid from each of the two freestreams in an asymmetric way*, even for equal freestream densities. In particular, for equal freestream densities ($s = 1$) and a freestream speed ratio of $r = 0.38$, Konrad estimated a volume flux entrainment ratio of $E_v \approx 1.3$. For a freestream density ratio of $s = 7$ (high speed He, low speed $N_2$) and the same velocity ratio, he estimated an entrainment ratio of $E_v \approx 3.4$.

Brown (1974) proposed an estimate for the entrainment based on the freestream velocity ratio, as seen from the frame of the large scale structures, i.e.,

$$E_v \approx r_c = \frac{U_1 - U_c}{U_c - U_2} \approx s^{1/2}$$

(cf. Eq. 13). Although the density ratio dependence of this proposal is in accord with the *ratio* of the two $E_v$ experimental estimates of Konrad, i.e., $3.4/1.3 \approx 2.6 \approx \sqrt{7}$, it cannot account for the asymmetric entrainment ratio that was observed with equal freestream densities.

This behavior can be understood in terms of the upstream/downstream asymmetry that a given large-scale vortical structure sees in a spatially growing shear layer and the fact, also noted by Fiedler (1975) in a different context, that a vortex entrains from each stream from its "lee side". See Fig. 13. For incompressible flow, simple arguments based on the symmetry of the flow in the large-scale structure convection frame (Dimotakis 1984), suggest that, for a similarly growing shear layer, the volume flux entrainment ratio can be estimated by the expression

$$E_v \approx \frac{U_1 - U_c}{U_c - U_2}\left(1 + \frac{\ell}{x}\right) , \tag{28}$$

where $\ell/x$ is the large-structure spacing-to-position ratio. In this expression, the quantity in parentheses is always greater than unity and the consequence of the spatial growth of the shear layer and the self-similarly increasing large-structure spacing with streamwise distance. It would be equal to unity for a temporally growing layer. Fitting the available data, one finds that the relation ($r = U_2/U_1$)

$$\frac{\ell}{x} \approx C_\ell \frac{1-r}{1+r} , \tag{29a}$$

with

$$C_\ell \approx 0.68 , \tag{29b}$$

is a good representation for $\ell/x$, independently of the freestream density ratio.

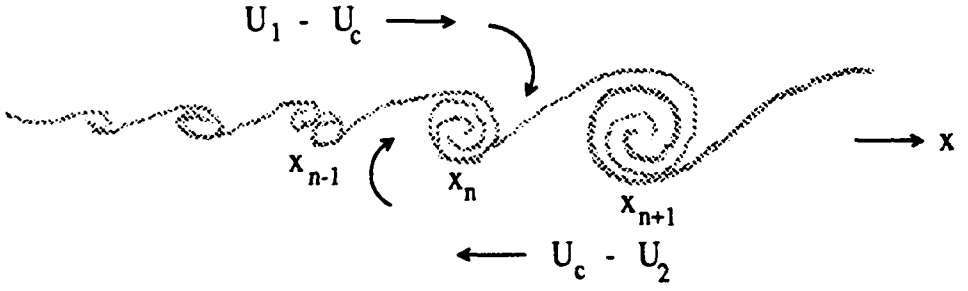


Fig. 13 Large-structure array and induction velocities in vortex convection frame.

We argued earlier that, for incompressible flow, $r_c = (U_1 - U_c)/(U_c - U_2) \approx s^{1/2}$. Consequently, for matched freestream densities and Konrad's freestream speed ratio of $r = 0.38$, we estimate (Eq. 28) that

$$E_v\,(r = 0.38,\, s = 1) \approx \left(1 + \frac{\ell}{x}\right) \approx 1.3 .$$

For the $He/N_2$ shear-layer data at the same speed ratio, we estimate that

$$E_v\,(r = 0.38,\, s = 7) \;\approx\; 7^{1/2} \times 1.3 \;\approx\; 3.4 \;.$$

Both estimates are in rather good agreement with Konrad's experimental values.

For incompressible flow, the *mass* flux entrainment ratio $E_m$ can also be similarly estimated, i.e.,

$$E_m \;=\; \frac{\rho_1}{\rho_2}\left(\frac{U_1 - U_c}{U_c - U_2}\right)\left(1 \;+\; \frac{\ell}{x}\right) \;, \tag{30a}$$

while for gas-phase flows, the *molar* entrainment ratio $E_n$ would be given by,

$$E_n \;=\; \frac{\mathcal{M}_2}{\mathcal{M}_1}\,E_m \;, \tag{30b}$$

where $\mathcal{M}_j$ denotes the molecular mass of the gas comprising the $j^{\text{th}}$ freestream.

The arguments that led to the expression for the entrainment ratio for incompressible flow (Eq. 28) should also be useful for compressible flow, noting that, in this case, $U_c$ must be computed accordingly (i.e., Eq. 14 or 18, as appropriate). Additionally, in the presence of shocks, one should not rely on the volumetric entrainment ratio $E_v$ but rather on the mass entrainment ratio $E_m$; the product $\rho u$ is conserved across a (normal) shock. Nevertheless, we recognize that in the presence of shocks borne by one freestream, or the other, but not both, the underlying symmetry of the flow, in the large-scale structure convection frame, is lost (e.g., Figs. 6). As a consequence, the correct expression for $E_m$ will also include an as yet undetermined multiplicative factor, of order unity, that captures this effect.

We can also expect that a revision of Eq. 29 for the spacing-to-position ratio $\ell/x$ would be necessary for compressible shear layers. A first guess is that $\ell/x$ might scale with $\delta/x$, as it does for subsonic flow, i.e.,

$$\frac{\ell}{x}[r,\, s;\, M_{c1}^{(i)} \to 0] \;\propto\; \frac{\delta}{x}[r,\, s = 1;\, M_{c1}^{(i)} \to 0] \;,$$

with a plausible extension of the form, as was assumed by Dimotakis and Hall (1987),

$$\frac{\ell}{x}[r,\, s;\, M_{c1}^{(i)}] \;\approx\; C_\ell\,\frac{1-r}{1+r}\,f[M_{c1}^{(i)}] \;, \tag{31}$$

where $f[\,M_{c1}^{(i)}\,]$ is an estimate of the Papamoschou and Roshko compressibility effect in the shear-layer growth, e.g., Eq. 17.

If one were to assess the relative importance of these different effects for compressible shear layers, one effect is likely to dominate. It is the asymmetry in the convective Mach numbers for flows that support shocks on one of the shear-layer freestreams (recall Fig. 5b) and the relative freestream speed ratio, $r_c$ (Eq. 22), in the turbulent-structure convective frame. This can be illustrated by considering the $M_1 = 1.5\,\mathrm{He}$, $M_2 = 0.3\,\mathrm{N_2}$ supersonic shear layer, documented by Hall *et al.* (1991a) by way of example. For this shear layer, we might have predicted a relative velocity ratio, based on an isentropic estimate for $U_c$, of

$$r_c^{(i)} = \frac{U_1 - U_c^{(i)}}{U_c^{(i)} - U_2} \simeq 2.1 \ . \tag{32a}$$

Instead, we have

$$r_c = \frac{U_1 - U_c}{U_c - U_2} \simeq 0.36 \ , \tag{32b}$$

using the convection velocity estimate of $U_c \approx 880\,\mathrm{m/s}$ that is suggested by the data and also derived using the stationary flow ansatz described earlier (see Dimotakis 1991 for more details). The two estimates of this important factor span unity and differ by a factor of 6. Such a layer, rather than being high-speed fluid rich may be *low*-speed fluid (depending on the other factors that enter in the entrainment ratio estimate).

In the context of mixing and the resulting range of mixed fluid compositions within the shear layer, it is useful to define a *conserved scalar* $\xi$ which denotes the mole fraction of high speed stream fluid in the molecularly mixed fluid (e.g., Bilger 1980). Accordingly, $\xi = 0$ corresponds to pure low-speed-stream fluid, $\xi = 1$ represents pure high-speed-stream fluid, and $\xi = 1/2$ represents a 50:50 mixture. In this notation, the entrainment ratio $E$ measures the flux of $\xi = 1$ fluid entering the turbulent mixing region, per unit flux of $\xi = 0$ fluid.

The asymmetric entrainment ratio suggests a zeroth order model for mixing in a two-dimensional shear layer, which entrains $\xi = 1$ and $\xi = 0$ fluid from each of the freestreams at a ratio $E$, respectively, that was employed by Konrad (1976) in his discussion of his concentration fluctuation data. The two entrained fluids are mixed by the efficient action of turbulence and can be expected to tend toward a mixed fluid composition of

$$\xi_E \equiv \frac{E_n}{E_n + 1} \ . \tag{33}$$

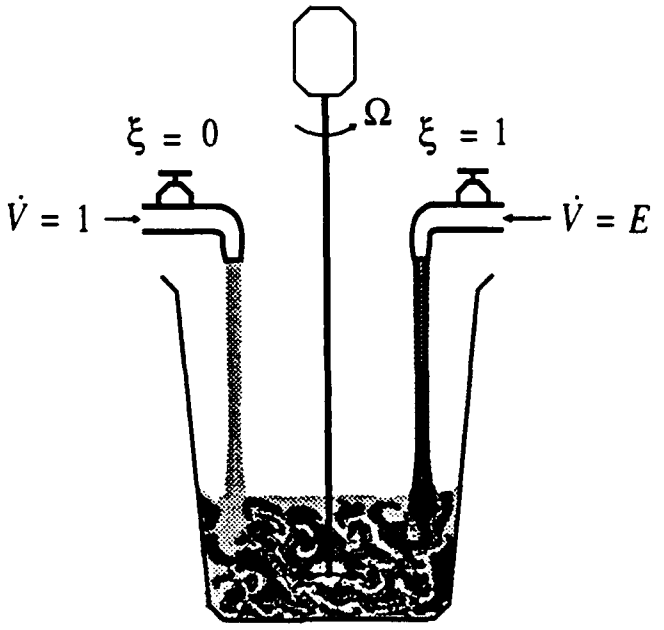


Fig. 14 Stirred bucket mixing. $E$ corresponds to the right/left faucet flow-rate ratio. Note that as the stirring rate is increased, at fixed faucet flow rate, $p(\xi)\,\mathrm{d}\xi \rightarrow \delta_{\mathrm{D}}(\xi - \xi_E)\,\mathrm{d}\xi$, where $\xi_E = E/(1+E)$.

A useful cartoon, depicted in Fig. 14, is that of a bucket being filled by two faucets running with unequal flow rates, as a laboratory stirring device mixes the effluents. We can also think of a hot/cold water faucet and the (average) temperature in the bucket; it is only a function of the ratio of the two flow rates. For all the complexity of the ensuing turbulent motion, we would expect to find a probability density function (PDF) of mixed fluid compositions in the bucket clustered around the value of the mixture fraction given by Eq. 33, where $E$ in our cartoon corresponds to the ratio of the flux from each of the two faucets. Fluid homogenized at this composition is an important component in the mixing model by Broadwell and Breidenthal (1982), as we will discuss below. One can appreciate that the range of compositions one should expect to encounter in the bucket depends on the relative rate of inflow to mixing. One can also appreciate that as we lower the combined faucet flow rate, keeping the ratio and the stirring fixed, we can expect the mixed fluid to be homogenized with a composition PDF tending to a Dirac delta function centered at $\xi_E$, i.e.,

$$p(\xi)\,\mathrm{d}\xi \;\rightarrow\; p_{\mathrm{H}}(\xi)\,\mathrm{d}\xi \;=\; \delta_{\mathrm{D}}(\xi - \xi_E)\,\mathrm{d}\xi \;, \tag{34}$$

in the limit. Similarly for a fixed faucet flow rate as the stirring rate is increased. See discussion, for example, in Levenspiel (1962).

The effects of the asymmetric entrainment ratio can be seen in the PDF measurements of made by Konrad (1976) in a gas-phase, matched freestream density ($\frac{1}{3}$ He : $\frac{2}{3}$ Ar) / $N_2$ shear-layer experiment, using an aspirating probe (Brown and Rebollo 1972). See Fig. 15. Note that the most probable value of the high speed fluid fraction $\xi$, denoted as $C(N_2)$ in the figure, is very close to $\xi_E \approx E/(1+E) = 0.57$, corresponding to the (independently) estimated matched density entrainment ratio of $E \approx 1.3$ (see Konrad 1976 for details).

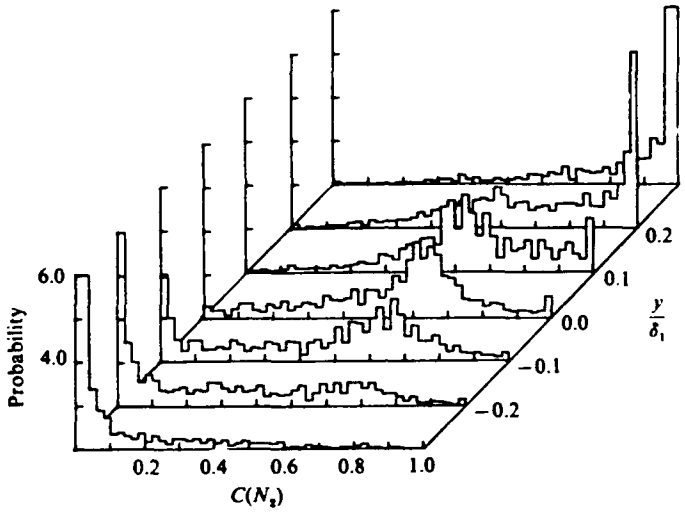


Fig. 15 Gas-phase PDF measurements in a matched density, $r = U_2/U_1 \approx 0.4$ shear layer beyond the mixing transition (Konrad 1976). High speed fluid mixture fraction $\xi$ is denoted by $C(N_2)$.

Similar measurements were obtained in water, in which the PDF was measured using laser-induced fluorescence techniques in a shear layer at the same velocity ratio (Koochesfahani and Dimotakis 1986). See Fig. 16. As can be seen, the most probable value of the composition is again very close to the $\xi_E \approx 0.57$ value.

Notable in both sets of measurements is the fact that this most probable value is observed *throughout* the shear layer. This can be understood in terms of the circumferential velocities, in the frame of the large-scale vortical structures, which can transport a fluid element from one side of the turbulent region to the other before it has much chance to alter its own internal mean composition. A comparison of the gas-phase and liquid-phase data suggests that, as expected at the higher Schmidt numbers in the latter case, this is more the case in the liquid than in the gas phase. It should be noted, however, that lower resolution in the gas-phase measurements could account for some of the observed trends.

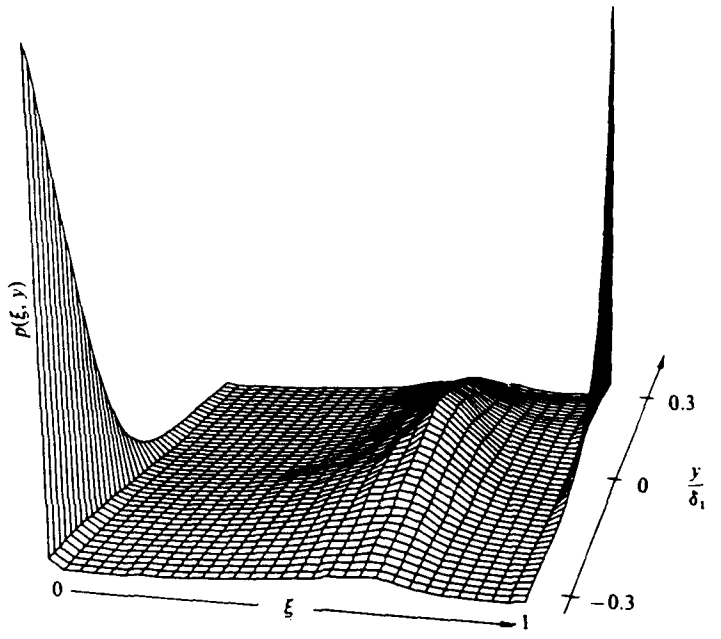


Fig. 16 High-speed fluid mixture fraction PDF measurements in a liquid-phase (matched density), $r = U_2/U_1 \approx 0.38$ shear layer at $Re = 2.3 \times 10^4$ (Koochesfahani and Dimotakis 1986). Plotted PDF computed from the run that yielded the post-mixing-transition image in Fig. 11).

These observations are at variance with the results of gradient-transport-based PDF modeling efforts (e.g., Pope 1981, Kollmann and Janicka 1982). Those models yield a most probable value of $\xi$ *for the mixed fluid* that is close to the local value of the mean mixture fraction profile (mixed and unmixed), i.e., $\overline{\xi}(y)$.

Important consequences of the asymmetric entrainment ratio, as reflected in the mixed fluid composition, are to be found in chemically reacting shear layers. In particular, in the case in which the reactant concentrations are not carried by the freestreams at the stoichiometric ratio, which side carries the *lean* reactant can make an easily discernible difference in the amount of chemical product formed in the layer. This was illustrated in the liquid-phase "flip" experiments of Koochesfahani *et al.* (1985) in which mixed fluid in the range of compositions $0 < \xi < 0.36$ was compared in a complementary run to mixed fluid in a range of compositions $0.64 < \xi < 1$, using a $pH$–sensitive, laser-induced fluorescence technique. See data in Fig. 17. The "chemical product" is found to be many times larger in the second case, which marks the high values of $\xi$ in the local composition. Note also that there is no systematic gradient in the labeled mixed fluid concentration across the shear-layer normalized width $\delta/x$. It should be emphasized that these experiments, which were designed to illustrate the potential of this effect, were

conducted in the mixing transition region, where the remnants of the much larger asymmetries in the initial roll-up have yet to be amortized with entrainment at the asymptotic values of the entrainment ratio (e.g., Eq. 28). See the pre-mixing-transition image in Fig. 11 data and Koochesfahani and Dimotakis (1986, Fig. 12 and related discussion). Similar conclusions were drawn by Masutani and Bowman (1986), from their gas-phase measurements in the mixing transition region, and by Sandham and Reynolds (1987), from the results of their computational modeling of the shear layer at low Reynolds number.

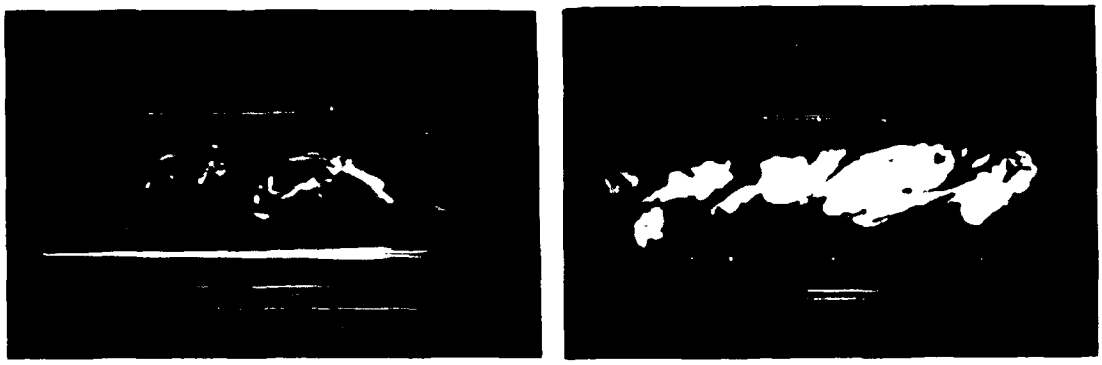

Fig. 17 Mixing transition laser-induced fluorescence "flip" experiment. Left picture: Fluorescence from mixed fluid compositions in the range $0 < \xi < 0.36$. Right picture: fluorescence from compositions in the range $0.64 < \xi < 1$ (from Koochesfahani *et al.* 1985).

A sufficient distance beyond the mixing transition, the observed asymmetries are consistent with the asymptotic values of $E$ and the associated "tilt" in the mixed fluid composition PDF in Fig. 16. See chemically reacting data at higher Reynolds numbers in Koochesfahani and Dimotakis (1986, Figs. 16 and 17). These and other mixing issues in subsonic turbulent shear layers will be discussed in the context of chemically reacting shear layers, which must be relied on for data at the high Reynolds numbers of interest here.

## 4. Chemical reactions: $\delta_P/\delta$

In the case in which the entrained fluids are not premixed and can react, the associated chemical product formation can obviously proceed no faster than the rate at which the reactants are mixed on a molecular scale by the turbulent flow. Considering a vertical slice of the turbulent region of streamwise extent $dx$, located at some downstream location $x$, the (expected) mixed fluid fraction $\delta_m/\delta$ within the transverse extent $\delta$ of the turbulent region occupied by molecularly mixed fluid (in the mean) represents an important upper bound for the expected chemical product fraction $\delta_P/\delta$ within the layer at that location. In the case of combustion of nonpremixed reactants, it also bounds the heat release corresponding to the amount of chemical product formed.

In the limit of fast chemistry, i.e., at a chemical kinetic rate sufficiently large so as not to serve as the limiting process in the rate of chemical product formation, the fraction of molecularly mixed fluid that is converted to chemical product, i.e., $\delta_P/\delta_m$, depends on the resulting PDF, i.e., $p(\xi)\,d\xi$, of molecular mixture compositions within the turbulent region. In particular, it depends on the distribution of mixture fractions $\xi$ of high-speed fluid to low-speed fluid in the molecularly mixed fluid, relative to the stoichiometric mixture fraction $\xi_\phi$ required for complete consumption of the available (entrained) reactants, as we will discuss later.

If the chemical kinetics are not sufficiently fast by the previous measure, the chemical product formation will lag behind the rate at which the reactants are mixed on a molecular scale by the turbulence. As a consequence, $\delta_P/\delta_m$ will be smaller, depending also on the ratio (Damköhler number)

$$Da \equiv \frac{\tau_m}{\tau_{ch}}\,, \tag{35}$$

of the expected time $\tau_m$ required for mixing, to the time $\tau_{ch}$ required to complete the ensuing chemical reactions. What is also important from a diagnostics vantage point is the recognition that, for chemical/flow systems that *can* be regarded as kinetically fast, i.e., in the limit of $Da \to \infty$, measurements of the chemical product volume fraction $\delta_P/\delta$ can be combined to provide us with reliable estimates of molecular mixing and the mixed fluid fraction $\delta_m/\delta$, as well as the distribution of compositions of the molecularly mixed fluid, as we will also discuss later. This often obviates the need for direct measurements of these quantities, which would, for the most part, have been anyway infeasible at the high Reynolds numbers of interest here. Direct computations fare no better, as the behavior of fast chemical systems can result in reaction zones that are even thinner than the expected diffusion scales (e.g., Eq. 26), under these conditions, and an intractably stiff problem numerically.

In the context of mixing, we will restrict the discussion that follows to the behavior in the limit of fast chemical kinetics ($Da \rightarrow \infty$). Chemical product formation for finite Damköhler numbers, however, is important theoretically inasmuch as it depends not only on the state of the flow at the measurement location but also on the flow history, which, in turn, prescribes the local molecular mixing (scalar dissipation) rate. See Bilger (1979, Sec. 2.5) and Williams (1988, Sec. 10.2.4) for a general discussion. It is also important from an applications vantage point, as the impetus for ever-increasing flight speeds is forcing us to consider chemical product formation at higher flow velocities and Mach numbers. In that regime, chemical product formation may, perforce, ultimately be limited by the fixed available chemical kinetic rates.

Data on the Damköhler number dependence of the product volume fraction in a gas-phase, subsonic shear layer were documented by Mungal and Frieler (1988). An analysis of these data in terms of the Broadwell-Breidenthal-Mungal model we will discuss later can be found in Broadwell and Mungal (1988). An attempt to incorporate a more realistic account of a complex chemical system was made by Dimotakis and Hall (1987), using the bucket zeroth-order mixing model described earlier (Fig. 14). The reader is directed to those references for an account.

## 4.1 Dependence on the stoichiometric mixture ratio

Consider the idealized case of the high-speed stream carrying a reactant at a concentration (mole fraction) $X_{01}$, and the low-speed stream carrying a reactant at a concentration $X_{02}$, which can react infinitely fast to form a chemical product, associated with an enthalpy release $\Delta\mathcal{H}$. An important quantity, in this context, is the *stoichiometric mixture ratio* $\phi$, defined as the volume (number of moles) of high speed fluid that carries sufficient reactants to consume a unit volume (mole) of low speed fluid, i.e.,

$$\phi \equiv \frac{X_{02}/X_{01}}{(X_{02}/X_{01})_{\rm st}} \,, \tag{36}$$

where the subscript "st" in the denominator denotes a stoichiometric mixture. For example, a (free-stream) stoichiometric mixture ratio of $\phi = 4$ implies that a mixture of four parts of high-speed fluid per part of low-speed fluid is required for complete consumption of all reactants. Accordingly, complete consumption of all reactants will occur at a stoichiometric (high speed fluid) mixture *mole fraction*

$$\xi_\phi = \frac{\phi}{\phi + 1} \,. \tag{37}$$

We can see that a mixture fraction of $\xi < \xi_\phi$, for example, will be lean in high-speed stream reactants and result in unreacted low-speed stream reactants. Similar definitions can also be employed on a mass basis (e.g., Kuo 1986, Sec. 1.8).

Consider, for example, the chemical reaction between hydrogen and fluorine which, in the limit of fast chemistry, we can simplify as a one-step reaction (see Mungal and Dimotakis 1984 for details)

$$H_2 + F_2 \longrightarrow 2\,HF\ , \qquad \Delta\mathcal{H} = -\,130\,\mathrm{kcal/mole}\ , \tag{38}$$

and which was used in many of the experiments that will be cited below. A mixture of $1\%\,H_2$ in $99\%\,N_2$ and an equal volume of $1\%\,F_2$ in $99\%\,N_2$ is stoichiometric and will result in an adiabatic (flame) temperature rise owing to the heat released of $\Delta T_f = 93\,\mathrm{K}$. A shear layer with a high-speed stream fluid composed of $4\%\,H_2 + 96\%\,N_2$, and a low-speed stream fluid of $1\%\,F_2 + 99\%\,N_2$ would be characterized by $\phi = 1/4$, i.e., $1/4$ parts of high-speed fluid must be mixed per part of low-speed fluid for complete reaction.

For equal heat and species diffusivities, i.e., for Lewis numbers $Le \equiv \kappa/\mathcal{D} = Sc/Pr = 1$, the adiabatic flame temperature rise $\Delta T_f(\phi)$ is the highest temperature rise that can be observed in the flow and serves as a convenient normalization of the observed mean temperature rise $\Delta T(y,\phi)$ in the reaction zone. Note that in a mixture in which $X_{01}$ is kept constant and the stoichiometric mixture ratio $\phi$ is changed by varying $X_{02}$ (Eq. 36), keeping the heat capacities constant in the process, the dependence of the adiabatic flame temperature rise on $\phi$ is given by

$$\Delta T_f(\phi) \;=\; \frac{2\phi}{\phi+1}\,\Delta T_f(1) \;=\; 2\,\xi_\phi\,\Delta T_f(1) \tag{39}$$

(recall Eq. 37).

Experimental data for the normalized mean temperature rise, for matched freestream density ($s = 1$), a freestream velocity ratio of $r \approx 0.4$, gas-phase reacting shear layers at low heat release, are plotted in Fig. 18 for $\phi = 1/8$, 1, and 8. The plotted quantity reflects the local mean fraction of the total chemical product (heat release) possible under the circumstances. There is a shift towards the lean side of the location of the peak mean temperature rise. There is also a marked asymmetry in the total amount of product (heat release) between the low-$\phi$ and the high-$\phi$ runs, which, in view of the relation between the entrainment ratio $E$ and the (required) stoichiometric mixture ratio $\phi$, is clear in this context. In particular, for

$\phi < E_n$, for example, fluid homogenized at the entrainment ratio will be low-speed stream reactant lean ($\xi_\phi < \xi_E$) and result in unconsumed high-speed stream reactants. The maximum amount of product is expected at $\phi \approx E_n$, with more product for $\phi \gg 1$ than for $\phi \ll 1$, for $E_n > 1$ (recall that $E_n \approx 1.3$ under these conditions). Note also that, consistent with our observation that a substantial fraction of fluid is unmixed within the shear layer, the mean temperature rise is everywhere less than $0.65\,\Delta T_f$.

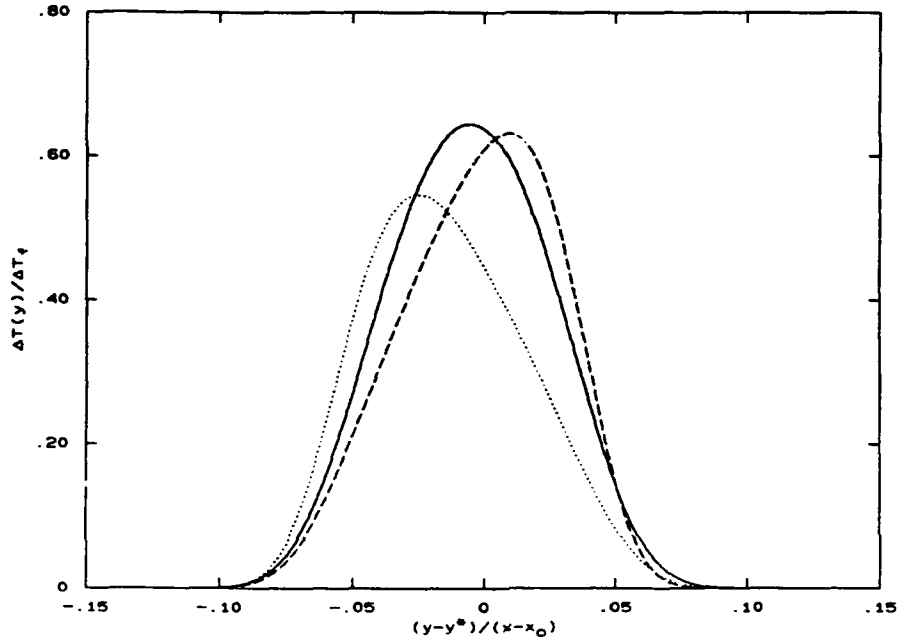


Fig. 18 Gas-phase shear layer: Normalized chemical product at low heat release. Solid line: $\phi = 1$; dashed line: $\phi = 8$; dotted line: $o = 1/8$ (Mungal and Dimotakis 1984; $s = 1$, $r \approx 0.4$). Note the peak temperature rise tilt towards the lean side for $\phi \neq 1$ and the larger total chemical product for $\phi \gg 1$ relative to $\phi \ll 1$, corresponding to an entrainment ratio of $E_n > 1$.

It is interesting to compare these results to the corresponding data from a liquid-phase ($s = 1$), chemically reacting shear layer, at the same freestream speed ratio ($r = 0.4$). These are depicted in Fig. 19, for $\phi = 1/10$ and $\phi = 10$. Note the reduced amount of product relative to the gas-phase results, the asymmetry between the high-$\phi$ and low-$\phi$ runs ($E_n \approx 1.3$ here also), but note that the tilt towards the lean side is no longer there. We can trace these differences to Schmidt number effects on the basis of our preceding discussions. In particular, the reduction in the total chemical product is attributable to the reduction in the amount of molecularly mixed fluid at the higher Schmidt number (lower species diffusivity). The absence

of a tilt of the peak mean temperature toward the lean side is the result of the delayed (slower) molecular mixing, which allows a longer Langrangian time for homogenization to occur at the larger-than-diffusion scales across the whole shear-layer transverse extent, owing to the large-structure motion (recall discussion of data in Fig. 16). See also discussion in Broadwell and Mungal (1988).

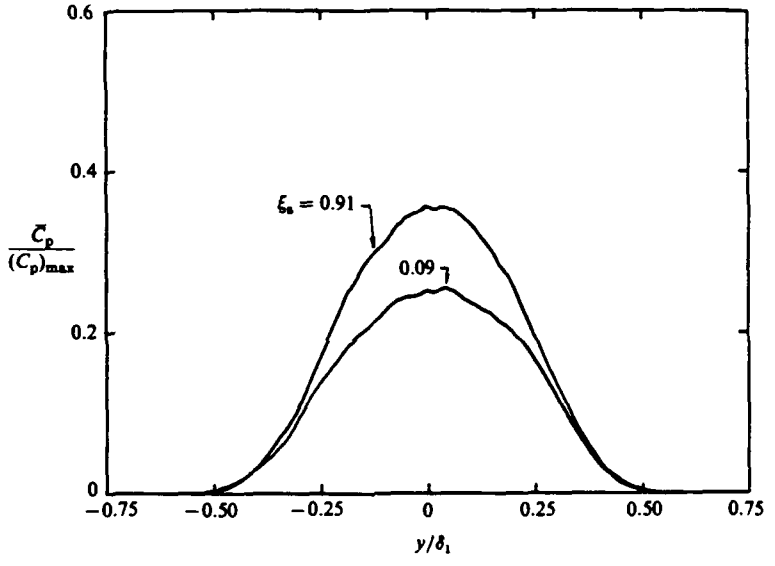


Fig. 19 Liquid-phase shear layer: Normalized chemical product at low heat release, for $\phi = 1/10, 10$ (Koochesfahani and Dimotakis 1986; $s = 1$, $r \approx 0.4$). Note symmetric chemical product distribution for both $\phi \gg 1$ and $\phi \ll 1$. $\xi_s$ in the figure denotes $\xi_\phi$ (Eq. 37).

## 4.2 Relation to the PDF. Schmidt number effects

These results would all be derivable from the local PDF $p(\xi, y)$ of the mixture fraction at the measuring station at $x$, if that were available. In particular, the product (or heat release) that can be produced corresponding to a particular value of the mixture fraction $\xi$ is easily computed by assuming complete consumption of the lean reactant. This yields two straight lines in $\xi$, joined at $\xi_\phi$, where the normalized product is equal to unity, i.e.,

$$\theta(\xi;\xi_\phi) = \begin{cases} \dfrac{\xi}{\xi_\phi}, & \text{for } 0 \le \xi \le \xi_\phi \ ; \\ \dfrac{1-\xi}{1-\xi_\phi}, & \text{for } \xi_\phi \le \xi \le 1 \end{cases} \tag{40}$$

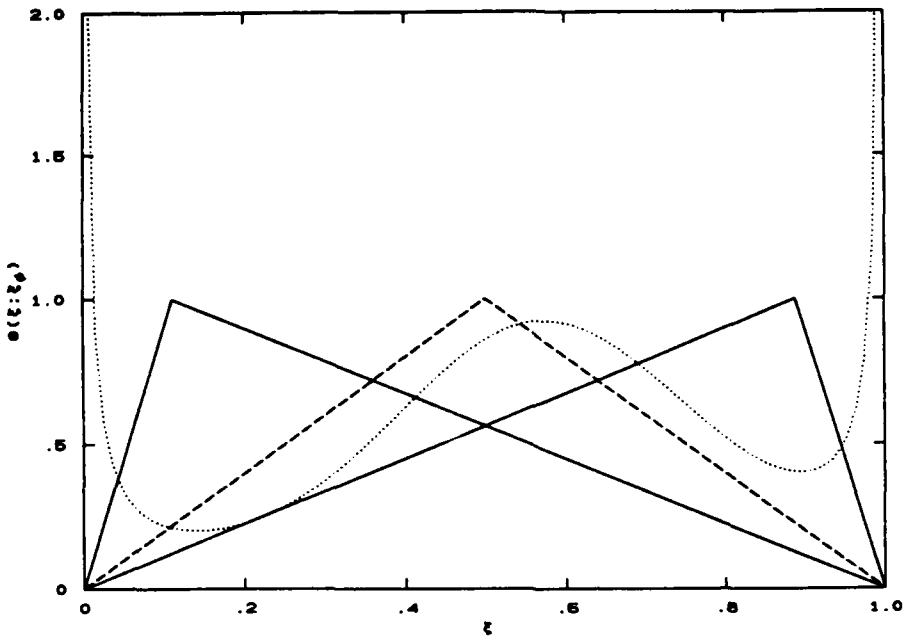


Fig. 20 Normalized chemical product function $\theta(\xi;\xi_\phi)$ for $\phi = 1/8$, and $\phi = 8$ (solid lines), and $\phi = 1$ (dashed line). PDF (dotted line) is sketched for reference, corresponding to $E_n \approx 1.3$ (cf. Fig. 18).

(see, for example, Kuo 1986, Sec. 1.9). This dependence is depicted in Fig. 20 for $\phi = 1/8$, 1, and 8.

The average chemical product volume (mole) fraction $\delta_P/\delta$ can be computed as the integral of the normalized product profile in the interior of the shear layer,

$$\frac{\delta_P(\xi_\phi)}{\delta} = \frac{1}{\delta}\int_{-\infty}^{\infty} \frac{\Delta T(y,\phi)}{\Delta T_f(\phi)}\,dy \ , \tag{41a}$$

or as an integral over the PDF of mixture fractions, since

$$\frac{\Delta T(y,\phi)}{\Delta T_f(\phi)} = \int_0^1 \theta(\xi;\xi_\phi)\,p(\xi,y)\,d\xi \ , \tag{41b}$$

where $\theta(\xi;\xi_\phi)$ is the triangular normalized product function (Eq. 40). Experimental values of this quantity are included in Fig. 21 for a gas-phase reacting shear layer at $Re = 6.4 \times 10^4$ (Mungal and Dimotakis 1984), as a function of the stoichiometric mixture fraction $\xi_\phi$. Also included in that figure is a point at $\phi = 10$ (Koochesfahani and Dimotakis 1986, $\xi_\phi = 0.91$) for a liquid-phase shear layer at a comparable Reynolds number ($Re = 7.8 \times 10^4$).

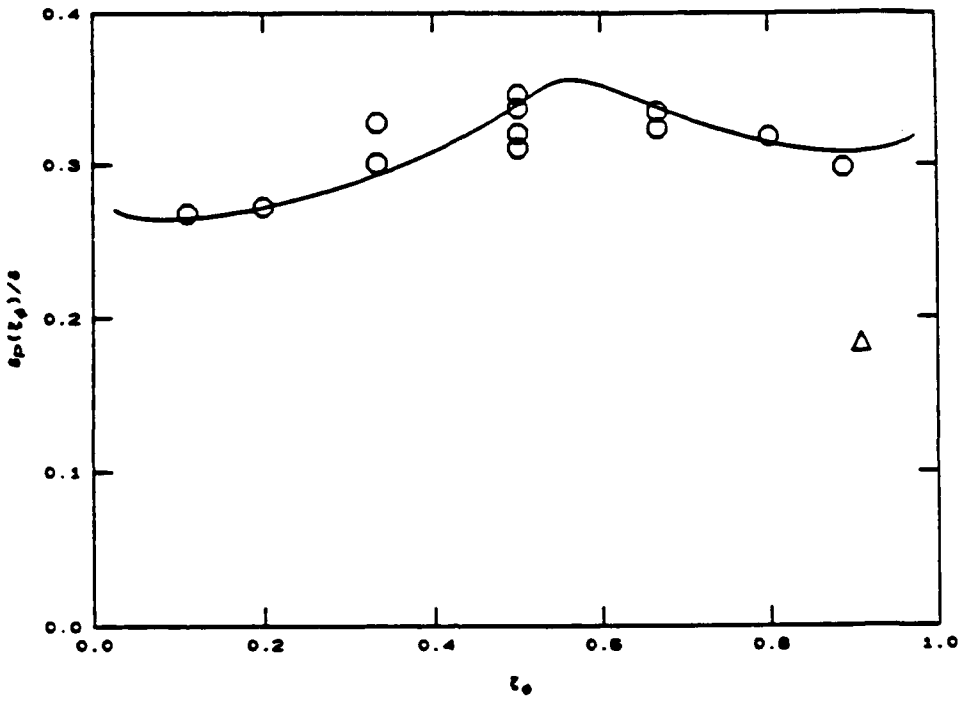


Fig. 21 Chemical product volume fraction $\delta_P/\delta$ vs. $\xi_\phi$ for $r \approx 0.4$ and matched freestream densities. Circles: gas-phase data (Mungal and Dimotakis 1984) $Re = 6.4 \times 10^4$. Triangle: liquid-phase data (Koochesfahani and Dimotakis 1986) $Re = 7.8 \times 10^4$. Smooth curve drawn to aid the eye.

The triangular normalized product function $\theta(\xi;\xi_\phi)$ suggests the use of chemically reacting experiments to estimate some statistics of the mixed fluid PDF. In particular, for $\xi_\phi \to 0$ and $\xi_\phi \to 1$, the ratio of the corresponding product volume fractions can be used to estimate the average composition $\overline{\xi}_m$ *in the mixed fluid*. For a small $\xi = \xi_0 \to 0$, we find

$$\overline{\xi}_m \approx \frac{\delta_P(1-\xi_0)}{\delta_P(\xi_0) + \delta_P(1-\xi_0)} . \tag{42}$$

Using the experimentally determined liquid-phase values of

$$\frac{\delta_P(\xi_\phi)}{\delta} = \begin{cases} 0.125 , & \text{at } \xi_\phi = \xi_0 = 0.09 ; \\ 0.165 , & \text{at } \xi_\phi = 1-\xi_0 = 0.91 , \end{cases} \tag{43}$$

we then estimate a value of $\overline{\xi}_m \approx 0.57$ (Koochesfahani and Dimotakis 1986). This agrees with the value of $\xi_E = E/(E+1)$, calculated using the independently estimated value of the volume flux entrainment ratio $E \simeq s^{1/2}(1+\ell/x) \approx 1.3$ (cf. Eqs. 28, 29, 13).

This idea was also used to estimate the dependence of the mean mixed fluid composition in a recent set of experiments (Frieler and Dimotakis 1988) in subsonic, low-heat-release, gas-phase shear layers with unequal freestream densities ($s \neq 1$), for which the expected asymmetries in the entrainment ratio can be large (Eqs. 13 and 28). The resulting data are plotted in Fig. 22 for freestream density ratios in the range of $0.1 < s < 4$, and compared to the estimated value of $\xi_E$, using the subsonic expression for the volume flux entrainment ratio discussed in the previous paragraph.

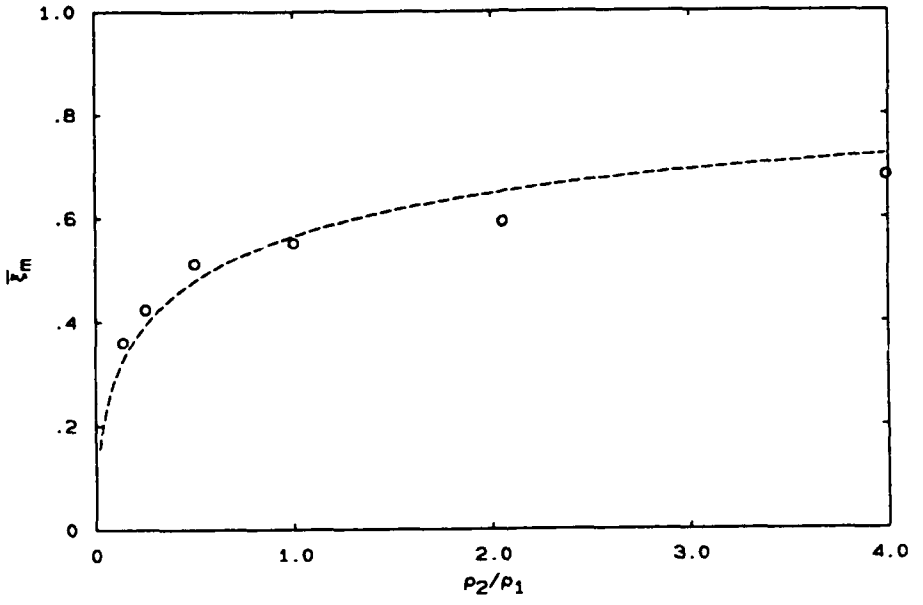


Fig. 22 Experimentally estimated mixed-fluid mixture fraction $\overline{\xi_m}$ as a function of the density ratio (Frieler and Dimotakis 1988). Dashed line depicts the estimated dependence of $\xi_E$ on the density ratio.

Comparing the triangular product functions for small and large $\xi_\phi$, we also note that, except for omitting the endpoints, they are essentially complements of each other. Consequently, for the case of negligible heat release, we find

$$\frac{\delta_m}{\delta} \approx (1-\xi_0)\left[\frac{\delta_P(\xi_0)}{\delta} + \frac{\delta_P(1-\xi_0)}{\delta}\right] .$$

This represents the mixed fluid fraction, if the edge contributions from the regions $0 < \xi < \epsilon$ and $1-\epsilon < \xi < 1$ are excluded from the mixed fluid tally. In this approximation, $\epsilon \approx \xi_0/2$, corresponding to the gas-phase chemical reaction product

function, and $\epsilon \approx \xi_0$ for the liquid-phase data. Using the values for the liquid-phase chemically reacting layer (Eq. 43), with $\epsilon \approx \xi_0 = 0.09$, we then estimate ($s = 1$)

$$\left(\frac{\delta_m}{\delta}\right)_{liq} \approx 0.26 \ . \tag{44a}$$

A similar calculation was also made using the results of the low-heat-release gas-phase data vs. freestream density ratio of Frieler and Dimotakis. Small dilatation corrections were applied to those data, which are of first order for this quantity. The results are plotted in Fig. 23 as a function of the freestream density ratio. It is significant that the mixed fluid fraction is found to be essentially independent of the density ratio, even as the mixed fluid composition depends rather strongly on it. The mixed fluid fraction derived from these data for matched freestream densities is then found to be (note that $\epsilon \approx \xi_0/2 \approx 0.05$)

$$\left(\frac{\delta_m}{\delta}\right)_{gas} \approx 0.49 \ . \tag{44b}$$

The estimates in Eqs. 44a and 44b were the values quoted in Eq. 27 for this quantity.

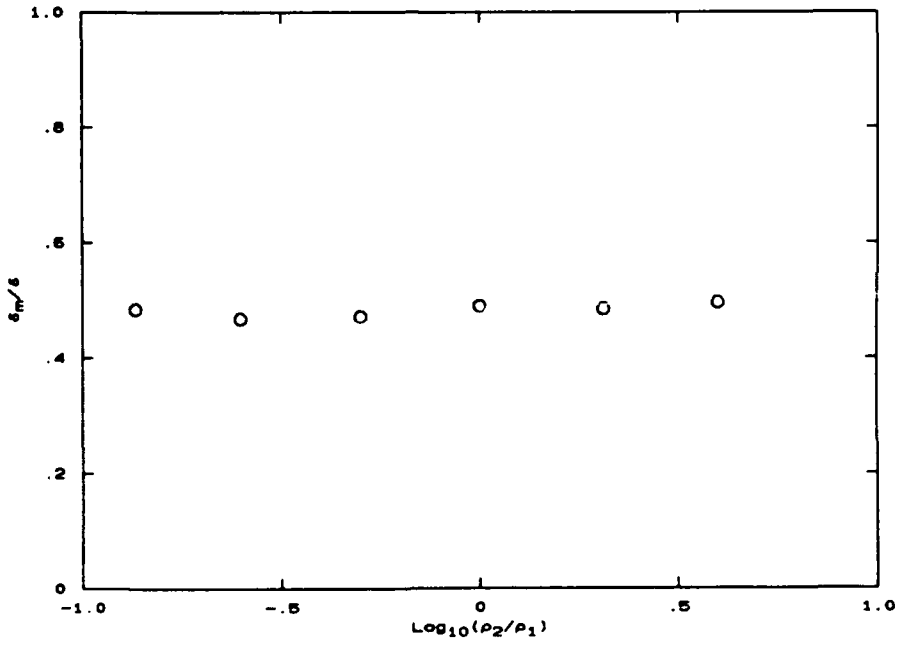


Fig. 23 Mixed fluid fraction $\delta_m/\delta$ as a function of the freestream density ratio $s = \rho_2/\rho_1$. Gas-phase data from Frieler and Dimotakis (1988).

### 4.3 Reynolds number effects

The existing experimental evidence suggests that chemical product formation and the resulting chemical product mole fraction $\delta_P/\delta$ observed at a station $x$ is a (weak) function of the local Reynolds number, at least for gas-phase flows. Available gas-phase and liquid-phase data, for a range of stoichiometric mixture ratio $\phi$, heat release (indicated by the adiabatic flame temperature rise $\Delta T_f$), and Mach number are plotted in Fig. 24 vs. $\log_{10}(Re)$.

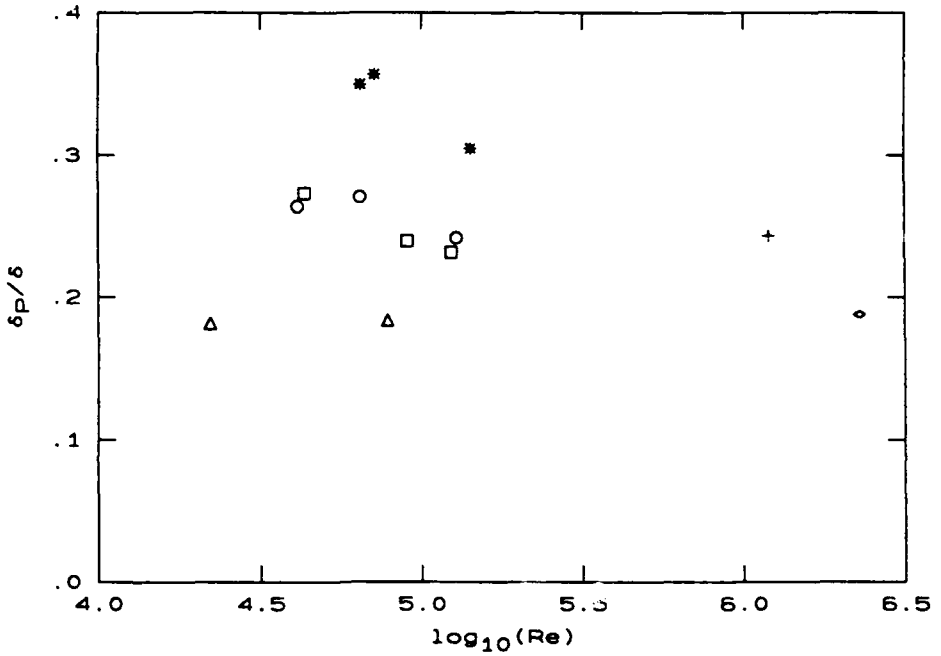


Fig. 24 Reynolds number dependence of chemical product mole fraction $\delta_P/\delta$. Subsonic gas-phase data: Circles (laminar boundary layer) and squares (turbulent boundary layer) from low-heat-release data of Mungal *et al.* (1985, $\phi = 1/8$, $\Delta T_f \approx 190\,\mathrm{K}$). Stars from the higher heat release data of Hermanson and Dimotakis (1989, $\phi = 1$, $\Delta T_f \approx 370\,K$). Supersonic shear-layer data (Hall *et al.* 1991b): Cross for $M_1 = 1.5\,N_2$, $M_2 = 0.3\,N_2$, $\phi = 1/4$, $\Delta T_f \approx 300\,\mathrm{K}$. Diamond for $M_1 = 1.5\,\mathrm{He}$, $M_2 = 0.3\,\mathrm{Ar}$, $\phi = 1/3$, $\Delta T_f \approx 580\,\mathrm{K}$. Liquid-phase data: Triangles from Koochesfahani and Dimotakis (1986, $\phi = 10$).

Although these data span a range of flow and chemical reaction parameters, one can discern by comparing results from a given set of conditions that for the gas-phase data, the product fraction $\delta_P/\delta$ is found to decrease slowly with increasing Reynolds number. Liquid-phase data exhibit an even weaker Reynolds number dependence,

if any, even though the lower Reynolds number value of $Re \approx 2.3 \times 10^4$ in those data may not be sufficiently above the mixing transition to be used for the comparison. The highest Reynolds number data included in the plot are derived from the recent measurements by Hall *et al.* (1991b) in supersonic shear layers. While it would appear that those values are consistent with the general trend, it is difficult to say, at this time, if the reason for the lower values of $\delta_P/\delta$ is attributable to the higher Reynolds numbers, or to compressibility. Further experiments, directed at separating these two important effects, are required.

It should be noted that the shear layer thickness $\delta$, at the measuring station $x$, was also changing with Reynolds number in these experiments. Although this variation was normalized out by taking the *ratio* of the product thickness $\delta_P$ and the shear layer (1%) thickness $\delta_{1\%} \approx \delta_{vis}$ to compute the chemical product mole fraction, we should appreciate that the change in the shear-layer thickness was sometimes larger than the change in the estimated product volume fraction documented in Fig. 24 (recall Figs. 2 and 3 and related discussion).

A proposal for an explanation of Reynolds number and Schmidt number effects was first made by Broadwell and Breidenthal (1982). The suggestion in that model was that the mixed fluid PDF can be modeled as a superposition of the $p_H(\xi)$ PDF corresponding to the homogeneously mixed fluid in the bucket cartoon and the contribution from thin interfacial diffusion layers interspersed in the shear layer, and which separate pure $\xi = 0$ and $\xi = 1$ fluid. Some revisions and clarifications were made in the more recent discussion of this model by Broadwell and Mungal (1988). The Broadwell-Breidenthal-Mungal (BBM) model then yields for the mixed fluid PDF, i.e., for $\xi \neq 0$ and $\xi \neq 1$,

$$p(\xi)\,d\xi \;\approx\; \left[ C_H\,\delta_D(\xi - \xi_E) \;+\; \frac{C_F}{\sqrt{Sc\,Re}}\,p_F(\xi) \right] d\xi \;, \qquad (45)$$

where $\delta_D(\xi)$ denotes the Dirac delta function and $p_F(\xi)$ is the PDF of composition as would arise in a laminar strained interface ("flame sheet") between $\xi = 0$ and $\xi = 1$ interdiffusing fluids. The dependence on the Reynolds number and Schmidt number in this superposition arises from modeling the amount of mixed fluid taken as residing in the diffusive interfaces. The coefficients $C_H$ and $C_F$ are assumed to be constants of the flow and, in particular, independent of the Schmidt and Reynolds numbers.

The proposed dependence on Schmidt number and Reynolds number in the BBM model is equivalent to the assumption that the interfacial diffusion-layer thicknesses can be modeled by scaling the relevant strain rate $\sigma$ using the local outer

flow variables, i.e., $\sigma \propto \Delta U/\delta$ (see Eq. 26), and that the associated diffusion interface surface-to-volume ratio is independent of the Reynolds number. These authors suggest that the model should apply for $Re \gg 1$, $\sqrt{Sc\,Re} \gg 1$, and $\sqrt{Re} \gg \ln Sc$, even though the latter inequality would automatically be satisfied at the Reynolds numbers of interest here (Broadwell and Mungal 1988).

Integrating the proposed model PDF over $\xi$, excluding the contributions of the unmixed fluid at $\xi = 0$ and $\xi = 1$, we then obtain, for the BBM model estimate of the mixed fluid fraction,

$$\frac{\delta_{\mathrm{m}}}{\delta} \approx C_{\mathrm{H}} + \frac{C_{\mathrm{F}}}{\sqrt{Sc\,Re}} \ . \tag{46}$$

A similar result is obtained for the product fraction $\delta_{\mathrm{P}}(\xi_\phi)/\delta$, in which the dependence of the homogeneous mixture contribution on $\xi_\phi$ is given by (see Eq. 40) $\theta(\xi_E;\xi_\phi)$, and the dependence of the flame sheet contribution is given by (see Broadwell and Mungal 1988)

$$F(\xi_\phi) = \frac{e^{-z_\phi^2}}{\sqrt{\pi}\,\xi_\phi\,(1-\xi_\phi)} \ , \tag{47a}$$

where the quantity $z_\phi$ is implicitly defined by the equation

$$\mathrm{erf}\, z_\phi = 2\left(\xi_\phi - \frac{1}{2}\right) \ . \tag{47b}$$

The constants $C_{\mathrm{H}}$ and $C_{\mathrm{F}}$ in the BBM model are to be determined by fitting the data, e.g., the Schmidt number dependence of $\delta_{\mathrm{m}}/\delta$ (Eq. 46). The proposed model PDF is depicted in Fig. 25, with the Dirac delta function contribution represented by a narrow Gaussian of the appropriate area, centered on a $\xi = \xi_E$ corresponding to an entrainment ratio of $E = 1.3$.

In the BBM estimates for $\delta_{\mathrm{m}}/\delta$ and $\delta_{\mathrm{P}}/\delta$, the "flame sheet" contribution vanishes at large Schmidt numbers (cf. Eq. 46). The gas/liquid difference is then accounted for by noting that the mixed fluid, in that case, is solely composed of the homogeneously mixed fluid at the composition $\xi \approx \xi_E$. Similarly, the gas-phase expressions asymptote to the liquid value at high Reynolds numbers. Conversely, the BBM model predicts that there should be no Schmidt number dependence at high Reynolds numbers. For gas phase flow, the predicted BBM dependence on Reynolds number is stronger ($Re^{-1/2}$) than the logarithmic dependence suggested by the data (Fig. 24) but nicely simulates the much weaker Reynolds number dependence of the liquid phase data. Finally, we should note that, according to the

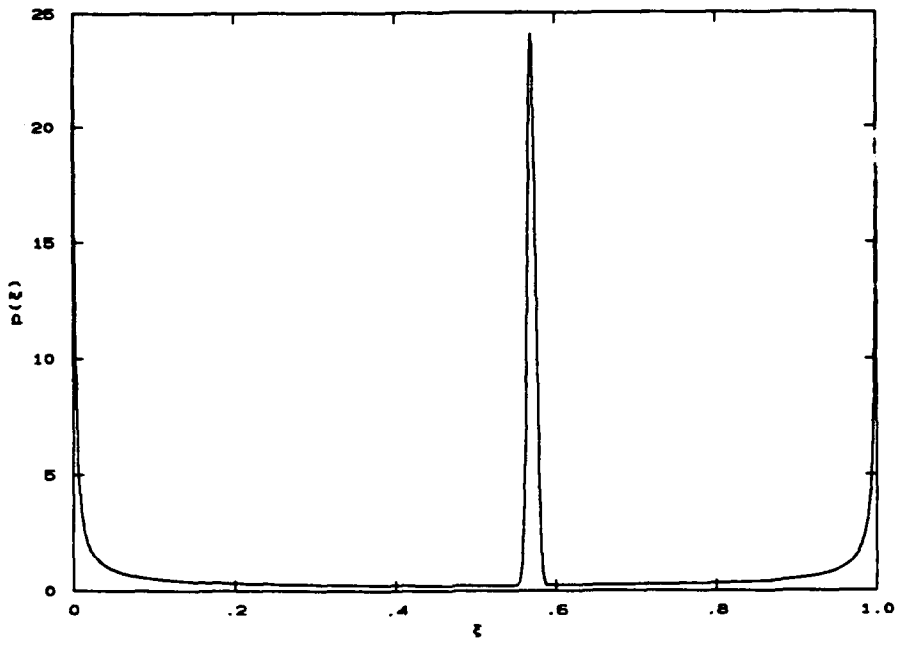


Fig. 25 Broadwell-Breidenthal-Mungal model PDF. See Broadwell and Breidenthal (1982).

BBM model, the mixed fluid and chemical product volume fraction does not depend on the fluid kinematic viscosity, being a function of the Peclet number,

$$Pe \equiv \frac{\Delta U\, \delta}{\mathcal{D}} = Sc \times Re \ ,$$

in which only the species diffusivity $\mathcal{D}$ enters. See Broadwell and Mungal (1988) for more details.

It is interesting that similar conclusions have also been arrived at by Kerstein (1988, 1989), using a phenomenological Monte Carlo model to represent the mechanics of turbulent transport and mixing. In his numerical simulations, Kerstein arrives at results for the mixed fluid and chemical product formed in a shear layer that are in accord with the BBM result expressed in the form of Eq. 46.

It could be argued that the strain rate at the interfacial surface formed by the turbulent flow between the entrained pure fluids from each of the freestreams should be estimated as a function of the distribution of spatial scales associated with that interface. In particular, one could argue that the predominant fraction of the surface-to-volume ratio $\mathcal{S}$ would be associated with the smallest scales in the flow which, for $Sc \approx 1$, would be in the vicinity of the Kolmogorov (1941) scale

$$\lambda_K \equiv \left(\frac{\epsilon^3}{\nu}\right)^{1/4} \ , \qquad (48a)$$

where $\varepsilon \propto (\Delta U)^3/\delta$ is the expected local kinetic energy dissipation rate per unit mass. This yields

$$\mathcal{S} \sim \frac{1}{\lambda_K} \sim \frac{1}{\delta} Re^{3/4} , \tag{49}$$

in the limit of large Reynolds numbers. The expected strain rate at those spatial scales would be proportional to the reciprocal of the Kolmogorov time $t_K \equiv \sqrt{\nu/\varepsilon}$ or, in terms of the outer variables of the flow,

$$\sigma_K \propto \frac{\Delta U}{\delta} Re^{1/2} . \tag{48b}$$

For $Sc \approx 1$, an estimate of the mixed fluid fraction scaling might be obtained as the product of the expected diffusion thickness $\lambda_\mathcal{D} \sim \sqrt{\mathcal{D}/\sigma}$ (Eq. 26), at the small scales, and the surface-to-volume ratio $\mathcal{S}$ of Eq. 49. It is interesting that this simple tally yields a *Reynolds-number-independent estimate*, to leading behavior, *for the mixed fluid fraction* (see also discussion in Dimotakis 1987, Sec. 3.3).

As a rebuttal to this argument, we recognize that the interfacial surface will be characterized by the full spectrum of turbulent scales and the associated distribution of strain rates. Accordingly, one might attempt a tally in which this distribution is accounted for, with closure requiring the assignment of a statistical weight to each scale $\lambda$ within the bounds of the turbulent flow. Such a model has been attempted (Dimotakis 1987), where it was argued that the statistical weight $w(\lambda)\,\mathrm{d}\lambda$ of a scale $\lambda$ in the self-similar inertial range must be given by

$$w(\lambda)\,\mathrm{d}\lambda \propto \frac{\mathrm{d}\lambda}{\lambda} , \tag{50}$$

as the only scale-invariant group that can be formed, and that the flow behavior below the Kolmogorov scale cannot alter this distribution in the range $\lambda_B < \lambda < \lambda_K$, where $\lambda_B = \lambda_K/\sqrt{Sc}$ is the scalar species Batchelor (1959) diffusion scale. This is equivalent to assuming that all scales are equally probable and that the statistical weight of a scale $\lambda$ is therefore given by the surface-to-volume ratio of that scale, i.e., $\mathcal{S}(\lambda) \propto 1/\lambda$, with the constant of proportionality determined by normalization This leads to an estimate for the mixed fluid fraction of

$$\frac{\delta_m}{\delta} \approx \frac{B_1(Sc)}{B_0(Sc) + \frac{3}{4}\left(1 - \frac{\mu}{8}\right)\ln(Re/Re_{cr})} , \tag{51}$$

where the functions $B_0(Sc)$ and $B_1(Sc)$ are determined by the calculation, $\mu \approx 0.3$ is the dissipation rate fluctuation coefficient, (Kolmogorov 1962, Oboukhov 1962), also known as the intermittency exponent (e.g., Monin and Yaglom 1975) and $Re_{cr} \approx 26$ (see Dimotakis 1987 for details).

The model predictions are in accord with the observed dependence of the chemical product on the stoichiometry of the free streams, as well as the Schmidt number and Reynolds number dependence of the chemical product and mixed fluid fractions. It also predicts an ever-decreasing chemical product and mixed fluid fraction with increasing Schmidt number (decreasing species diffusivity). As can be seen in the resulting expression for $\delta_m/\delta$, however, it predicts that the mixed fluid volume fraction is also an ever-decreasing (albeit slowly) function of the Reynolds number. This is a rather robust consequence of the $w(\lambda)\,d\lambda$ statistical weight distribution that was assumed (Eq. 50). On the other hand, even a small departure from this distribution would alter this behavior in the limit, with no discernible differences within the range of Reynolds numbers that have been investigated and are typically achievable in the laboratory.

It need not be emphasized that the dependence and limiting behavior of turbulent mixing processes on Reynolds number is of considerable significance not only theoretically but also from an applications vantage point.

## 5. Discussion and conclusions

For all the progress that has been made in addressing problems of mixing and combustion in turbulent shear flows, it is clear that important issues remain to be resolved. Many of these arise from the complexity and constraints imposed on these flows for a diverse set of reasons, which fundamental research often has the luxury of ignoring. Just as significant, however, are the problems that can be considered important and fundamental from any perspective, whose resolution would not only advance our understanding of turbulence, mixing, and combustion but would also have a direct impact on technology and applications. As Boltzmann used to say: "There is nothing more practical than a good theory."

Of the many problems that emerge from the preceding discussion, there are three, in my opinion, that merit close future scrutiny. These are: the apparent dependence of the far field behavior of high Reynolds number flows on initial conditions, the limiting behavior of high Reynolds number turbulence as the Reynolds number is increased to very large values, and the nature of turbulence under compressible flow conditions. The discussion that follows on these is necessarily more in the nature of speculation. In deference to Sir Arthur's admonition: "It is dangerous to theorize without data."

To paraphrase one of the conclusions of the discussion on shear-layer growth, it is surprising that the initial conditions seem to determine what appears to be the asymptotic behavior of the turbulent shear layer. Should that interpretation survive future scrutiny, it must be considered a remarkable manifestation of what the equations of motion are clearly capable of admitting in principle. Nevertheless, it flies in the face of traditional assumptions about the behavior of turbulence in the limit of high Reynolds numbers. Additionally, unless an explanation and an accounting can be formulated for this behavior, it also complicates the analysis, simulation, and modeling of these flows in that this behavior will appear as a nonunique response to seemingly similar flow conditions. To the extent that we cannot mix any faster than the shear layer grows, the stakes, both theoretically and from an applications standpoint, are not small, as measured by the range of empirical values of the shear layer growth coefficient $C_\delta$ of almost a factor of 2 (recall Eqs. 10, 11).

Turning the coin over, we can see the potential for substantial benefits from flow control: if we can get, or ...lose, a factor of 2 by doing hardly anything, think what we can do if we try! Some recent results in our laboratory in what has previously been regarded as canonical turbulent jet mixing also substantiate this

conclusion (see Miller 1991, Ch. 6) and suggest that this behavior is not peculiar to shear layers. There is a growing body of evidence that the possibilities that arise with active flow control are very significant, as can be seen from the work cited on the response of shear layers to external forcing (footnote, Sec. 2.1), the flow control in jets (Parekh and Reynolds 1989), the flow control and resulting mixing control in the wake of a circular cylinder (Tokumaru and Dimotakis 1991), and many others that have not been included here.

Returning to shear layers, it is important to understand the mechanism by which the initial conditions are felt by the flow thousands of momentum thicknesses downstream of the splitter plate trailing edge and how this observation is reconcilable with classical theories and descriptions of turbulence. It will be interesting to examine this issue and the clues that may be offered by the various research efforts in supersonic shear layers in progress. As the flow changes from elliptic to hyperbolic, the communication channels between different portions of the flow become a function of the Mach number of the two streams, as well as the respective convective Mach numbers that result.

In considering Reynolds number effects, it may be useful to think about a *gedanken* experiment in which the Reynolds number is varied by controlling the test section or combustor *pressure* at fixed geometry and freestream speeds. This would control the Reynolds number (at fixed Schmidt number) through a change in the molecular diffusivity coefficients, leaving most other flow parameters unaltered. Such a scheme would still change the Reynolds number of the initial conditions (recall Figs. 2 and 3, related caveats, and previous discussion), as well as the expected number of large-scale structures between the splitter-plate trailing edge and a fixed measuring station (Dimotakis and Brown 1976). Nevertheless, it would leave the scaling with respect to the local *outer* flow variables unaltered and make it easier to argue for (or even discern, should such experiments be undertaken in the future) the subtle dependence of turbulence and mixing on the fluid Reynolds number, at fixed Schmidt number. If the dynamic range of Reynolds numbers in such experiments is large enough, one might obtain important clues about the behavior of turbulence as the Reynolds number is increased without limit. This is all the more important because the experimental evidence suggests that the mixed fluid fraction in shear layers is decreasing with increasing Reynolds number, in a Reynolds number regime untouchable by the foreseeable computing community, most models silent on the issue, and disagreement between two models that have stuck their necks out at this writing!

To complicate matters further, we should mention that recent experimental investigations of turbulent mixing in turbulent jets in our laboratory, in both gas-phase and liquid-phase flows, suggest that the dependence of turbulent *jet* mixing on Reynolds number *has the opposite sign*. Specifically, we have found that, for gas-phase flows, turbulent jet diffusion flame length *decreases* with Reynolds number, up to a jet Reynolds number of $Re \approx 2.5 \times 10^4$, indicating better mixing in the far field with increasing Reynolds number for turbulent jets. The near field behavior is more complicated, as evidenced by the Reynolds number dependence of the virtual origin of the jet flame length with respect to stoichiometric mixture ratio (Gilbrech 1991). Measurements in liquid-phase jets have shown similar trends, as manifested by a *decreasing* variance of the jet fluid concentration fluctuations in the far field of the jet with increasing Reynolds number, with no Reynolds-number-independent mixing regime, beyond some minimum Reynolds number, at least within the range of Reynolds numbers attained in the experiments (Miller and Dimotakis 1991, Miller 1991). These results are very significant, in light of the opposite behavior found for shear layers, because they suggest that *the dependence of turbulent mixing processes on Reynolds number is not universal.* This behavior can probably be traced to differences in the behavior at the largest flow scales and the interplay between the large-scale organized structures, that are manifestly peculiar to each flow geometry, and the behavior at the smallest small scales, where the actual molecular mixing largely takes place. It goes without saying that this behavior must also be captured by turbulent mixing models, if they are to account for the observed phenomena.

Even in the unlikely event that compressible turbulence proves to be an even better mixer than its incompressible counterpart, it seems clear that we should expect to find a reduced overall mixing rate at high Mach numbers relative to incompressible flow. If the growth rate, absent external disturbances and mixing devices, is diminished by a factor of five, or so, there is little the turbulent interior can do to offset this reduction. In fact, the scant experimental evidence presently available from chemically reacting experiments in supersonic shear layers (see Fig. 24) would indicate that one should probably not expect any spectacular surprises on this score from canonical shear-layer flow configurations.

A second potentially important difference in behavior can be gleaned from the discussion of the entrainment ratio and the behavior of the large scale structure convection velocity under supersonic conditions. In particular, in a flow regime where the evidence and simple arguments suggest that shocks may be borne by one free stream or another, but not both, we expect much larger potential asymmetries in the entrainment ratio than in incompressible flow. To make matters worse, it

is possible that it may prove difficult to predict or control in which direction the asymmetry may be realized. This is of considerable significance in the context of the expected composition of the mixed fluid, to the extent that one may not be able to predict and design for even the stoichiometry at which the combustion may have to be asked to take place within a shear layer zone. Moreover, it is a behavior that may well exhibit large changes in response with small changes in Mach number.

As for the mixing process itself, we can only speculate about it, at present. Our views of compressible turbulence are limited and not well substantiated. Some of the mainstays of incompressible turbulence, like the Kolmogorov similarity theories, may have to be revised if not abandoned as supersonic convective Mach numbers admit shocks running through the flow. There is evidence that in cases in which the driving field can generate eddies at intermediate scales, these similarity ideas cease to apply. In the case of shocks running through a turbulent flow characterized by density inhomogeneities, baroclinic generation of vorticity will form such eddies (e.g., Haas and Sturtevant 1987, Brouillette 1989, Waitz 1991, Yang 1991), which will both influence and be influenced by subsequent shocks that visit (e.g., Hesselink and Sturtevant 1988, Rotman 1991). Secondly, in an environment that is characterized by limits in the *speed*, on the one hand, and couples density fluctuations particularly efficiently to acoustically radiated power, as the Mach number increases, fluctuations and mixing may become dear commodities. On the other hand, this behavior could depend rather strongly on whether this is confined or open flow, as noted in our discussion on stability analysis (Tam and Morris 1980, Tam and Hu 1988, Sec. 2.2) and by H. Hornung in private discussions, with the *sign* of the outcome possibly dependent on the details!

It may be worth concluding by stating what is perhaps obvious, namely, that, from an applications point of view, *enhancement* of shear-layer growth and mixing is not always the objective. Although it may be, if one is interested in combustion efficiency and propulsion, it certainly is not the objective in the case of film cooling of hypersonic propulsion devices, aerodynamic windows for high-power chemical lasers, etc. What is at a premium here is the mastering of the fundamental physics of these phenomena, which will permit the optimization and control of their behavior, in each case, for the specific, complex, and sometimes purposes unanticipated at the outset.

## 6. Acknowledgments

I would like to acknowledge the continuous discussions within the GALCIT community, which directly or indirectly have contributed to the work reviewed and to this paper. I would, however, specifically like to recognize the many, often heated, discussions with Dr. J. Broadwell over the years, which have contributed to this work and the evolution of the ideas described in this discussion. I would also like to thank Mr. C. Frieler for his help with the preparation of some of the figures. Finally, I would like to acknowledge the many contributions and expertise of Dr. Dan Lang, who has been responsible for many of the electronics and computer-data-acquisition developments throughout the experimental effort at GALCIT summarized in this paper, without which many of the experiments would have had to wait for the corresponding capabilities to have become available commercially.

This work is part of a larger effort to investigate mixing and combustion in turbulent shear flows, sponsored by the Air Force Office of Scientific Research Contract No. F49620-79-C-0159 and Grants AFOSR-83-0213 and AFOSR-88-0155, whose support is gratefully acknowledged.

## 7. References

ABRAMOWICH, G. N. 1963, *The Theory of Turbulent Jets* (MIT Press, Cambridge, MA).

ALVAREZ, C., AND MARTINEZ-VAL, R. 1984, "Visual measurement of streamwise vorticity in the mixing layer," *Phys. Fluids* **27**(9), 2367–2368.

BATCHELOR, G. K. 1959, "Small-scale variation of convected quantities like temperature in turbulent fluid. Part 1. General discussion and the case of small conductivity," *J. Fluid Mech.* **5**, 113–133.

BATT, R. G. 1975, "Some Measurements on the Effect of Tripping the Two-Dimensional Shear Layer," *AIAA J.* **13**(2), 245–247.

BERNAL, L. P. 1981, *The Coherent Structure of Turbulent Mixing Layers. I. Similarity of the Primary Vortex Structure, II. Secondary Streamwise Vortex Structure*, Ph.D. thesis, California Institute of Technology.

BERNAL, L. P., BREIDENTHAL, R. E., BROWN, G. L., KONRAD, J. H., AND ROSHKO, A. 1979, "On the Development of Three-Dimensional Small Scales in Turbulent Mixing Layers," $2^{nd}$ *Int. Symposium on Turb. Shear Flows.* (Springer-Verlag, New York, 1980), 305–313.

BERNAL, L. P., AND ROSHKO, A. 1986, "Streamwise vortex structure in plane mixing layers," *J. Fluid Mech.* **170**, 499–525.

BERS, A. 1975, "Linear waves and instabilities," *Physique des Plasmas* (edited by C. DeWitt and J. Peyraud, Gordon and Breach, New York), 117–213.

BILGER, R. W. 1979, "Turbulent Jet Diffusion Flames," *En. and Comb. Science* (Student Ed. **1**, N. Chigier, ed.), 109–131.

BILGER, R. W. 1980, "Turbulent Flows with Nonpremixed Reactants," *Turbulent Reacting Flows* (Springer-Verlag, Topics in Applied Physics **44**, Eds. P. A. Libby, F. A. Williams, New York), 65–113.

BILGER, R. W. 1989, "Turbulent Diffusion Flames," *Ann. Rev. Fluid Mech.* **21**, 101–135.

BOGDANOFF, D. W. 1983, "Compressibility Effects in Turbulent Shear Layers," *AIAA J.* **21**(6), 926–927.

BRADSHAW, P. 1966, "The Effect of Initial Conditions on the Development of a Free Shear Layer," *J. Fluid Mech.* **26**(2), 225–236.

BREIDENTHAL, R. E. 1981, "Structure in Turbulent Mixing Layers and Wakes Using a Chemical Reaction," *J. Fluid Mech.* **109**, 1–24.

BRIGGS, R. J. 1964, "Electron-stream interaction in plasmas," Research Monograph No. 29 (M.I.T. Press, Cambridge, MA).

BROADWELL, J. E., AND BREIDENTHAL, R. E. 1982, "A Simple Model of Mixing and Chemical Reaction in a Turbulent Shear Layer," *J. Fluid Mech.* **125**, 397–410.

BROADWELL, J. E., AND MUNGAL, M. G. 1988, "Molecular Mixing and Chemical Reactions in Turbulent Shear Layers," 22nd *Symposium (International) on Combustion* (The Combustion Institute, Pittsburgh), 579–587.

BROUILLETTE, M. 1989, *On the Interaction of Shock Waves with Contact Surfaces Between Gases of Different Densities*, Ph.D. thesis, California Institute of Technology.

BROWAND, F. K. 1986, "The Structure of the Turbulent Mixing Layer," *Physica* D **18**, 135–148.

BROWAND, F. K., AND LATIGO, B. O. 1979, "Growth of the Two-Dimensional Mixing Layer from a Turbulent and Non-Turbulent Boundary Layer," *Phys. Fluids* **22**(6), 1011–1019.

BROWN, G. L. 1974, "The Entrainment and Large Structure in Turbulent Mixing Layers," Proceedings, 5th *Australasian Conf. on Hydraulics and Fluid Mechanics*, 352–359.

BROWN, G. L., AND REBOLLO, M. R. 1972, "A Small, Fast-Response Probe to Measure Composition of a Binary Gas Mixture," *AIAA J.* **10**(5), 649–652.

BROWN, G. L., AND ROSHKO, A. 1971, "The Effect of Density Difference on the Turbulent Mixing Layer," *Turbulent Shear Flows*, AGARD–CP–93, 23.1–12.

BROWN, G. L., AND ROSHKO, A. 1974, "On Density Effects and Large Structure in Turbulent Mixing Layers," *J. Fluid Mech.* **64**(4), 775–816.

CHINZEI, N., MASUA, G., KOMURO, T. MURAKAMI, A., AND KUDOU, K. 1986, "Spreading of two-stream supersonic turbulent mixing layers," *Phys. Fluids* **29**(5), 1345-1347.

CLEMENS, N. T., AND MUNGAL, M. G. 1990, "Two- and Three-Dimensional Effects in the Supersonic Mixing Layer," AIAA Paper 90–1978.

COLES, D. 1981, "Prospects for Useful Research on Coherent Structure in Tur-

bulent Shear Flow," *Proc. Indian Acad. Sci. (Eng. Sci.)* **4**(2), 111–127.

COLES, D. 1985, "Dryden Lecture: The Uses of Coherent Structure," *AIAA* 23rd *Aerospace Sciences Meeting*, AIAA Paper 85–0506

CORCOS, G. M., AND LIN, S. J. 1984, "The mixing layer: deterministic models of the turbulent flow. Part 2. The origin of the three-dimensional motion.," *J. Fluid Mech.* **139**, 67–95.

CORCOS, G. M., AND SHERMAN, F. S. 1984, "The mixing layer: deterministic models of the turbulent flow. Part 1. Introduction and the two-dimensional flow," *J. Fluid Mech.* **139**, 29–65.

DAILY, J. W., AND LUNDQUIST, W. J. 1984, "Three dimensional structure in a turbulent combusting mixing layer," $20^{th}$ *Symposium (International) on Combustion* (The Combustion Institute, Pittsburgh), 487–494.

DEMETRIADES, A. 1980, "Necessary conditions for transition in a free shear layer," AFOSR–TR–80–0442.

DEMETRIADES, A., AND BROWER, T. L. 1982, "Experimental Study of Transition in a Compressible Shear Layer," Montana State U. Annual Report, AFOSR–TR–83–0144.

DEMETRIADES, A., ORTWERTH, P. J., AND MOENY, W. M. 1981, "Laminar-Turbulent Transition in Free Shear Layers," *AIAA J.* **19**(9), 1091–1092.

DIMOTAKIS, P. E. 1984, "Two-dimensional shear-layer entrainment," *AIAA* 22nd *Aerospace Sciences Meeting*, *AIAA J.* **24**(11), 1791–1796 (1986).

DIMOTAKIS, P. E. 1987, "Turbulent shear layer mixing with fast chemical reactions," US-France Workshop on Turbulent Reactive Flows. *Turbulent Reactive Flows* (Springer-Verlag, New York, 1989), 417–485.

DIMOTAKIS, P. E. 1991, "On the convection velocity of turbulent structures in supersonic shear layers," *AIAA* 22nd *Fluid Dynamics, Plasma Dynamics and Lasers Conference* , AIAA Paper 91–1724.

DIMOTAKIS, P. E., AND BROWN, G. L. 1976, "The Mixing Layer at High Reynolds Number: Large-Structure Dynamics and Entrainment," *J. Fluid Mech.* **78**(3), 535–560 + 2 plates.

DIMOTAKIS, P. E., AND HALL, J. L. 1987, "A simple model for finite chemical kinetics analysis of supersonic turbulent shear layer combustion," AIAA/SAE/-

ASME/ASEE 23rd Joint Propulsion Meeting , AIAA Paper 87–1879.

DZIOMBA, B., AND FIEDLER, H. E. 1985, "Effect of initial conditions on two-dimensional free shear layers," *J. Fluid Mech.* **152**, 419–442.

FIEDLER, H. E. 1975, "On Turbulence Structure and Mixing Mechanism in Free Turbulent Shear Flows," *Turbulent Mixing in Non-Reactive and Reactive Flows* (Plenum Press, New York), 381–409.

FOURGUETTE, D., MUNGAL, M. G., AND DIBBLE, R. 1990, "Time Evolution of the Shear Layer of an Axisymmetric Supersonic Jet at Matched Conditions," *AIAA 28th Aerospace Sciences Meeting*, AIAA Paper 90–0508.

FRIELER, C. E., AND DIMOTAKIS, P. E. 1988, "Mixing and Reaction at Low Heat Release in the Non-Homogeneous Shear Layer," *First National Fluid Dynamics Congress*, AIAA Paper 88–3626.

GANJI, A. R., AND SAWYER, R. F. 1980, "Experimental Study of a Two-Dimensional Premixed Turbulent Flame," *AIAA J.* **18**(7), 817–824.

GILBRECH, R. J. 1991, *An Experimental Investigation of Chemically-Reacting, Gas-Phase Turbulent Jets*, Ph.D. thesis, California Institute of Technology.

GROPENGIESSER, H. 1970, "Study of the Stability of Boundary Layers in Compressible Fluids," NASA–TT–F–12, 786.

HAAS, J. F., AND STURTEVANT, B. 1987, "Interaction of weak shock waves with cylindrical and spherical gas inhomogeneities," *J. Fluid Mech.* **181**, 41–76.

HALL, J. L. 1991, *An Experimental Investigation of Structure, Mixing and Combustion in Compressible Turbulent Shear Layers*, Ph.D. thesis, California Institute of Technology.

HALL, J. L., DIMOTAKIS, P. E., AND ROSEMANN, H. 1991a, "Experiments in non-reacting compressible shear layers," *AIAA 29th Aerospace Sciences Meeting*, AIAA Paper No. 91–0629.

HALL, J. L., DIMOTAKIS, P. E., AND ROSEMANN, H. 1991b, "Some measurements of molecular mixing in compressible turbulent mixing layers," *AIAA 22nd Fluid Dynamics, Plasma Dynamics and Lasers Conference* , AIAA–91–1719.

HERMANSON, J. C., AND DIMOTAKIS, P. E. 1989, "Effects of heat release in a turbulent reacting shear layer," *J. Fluid Mech.* **199**, 333–375.

HESSELINK, L., AND STURTEVANT, B. 1988, "Propagation of weak shocks through

a random medium," *J. Fluid Mech.* **196**, 513–553.

HO, C.-M., AND HUERRE, P. 1984, "Perturbed Free Shear Layers," *Ann. Rev. Fluid Mech.* **16**, 365–424.

HUERRE, P., AND MONKEWITZ, P. A. 1985, "Absolute and convective instabilities in free shear layers," *J. Fluid Mech.* **159**, 151-168.

HUSAIN, Z. D., AND HUSSAIN, A. K. M. F. 1983, "Natural Instability of Free Shear Layers," *AIAA J.* **21**(11), 1512–1517.

HUSSAIN, A. K. M. F. 1977, "Initial Condition Effect on Free Turbulent Shear Flows," Proceedings, *Structure and Mechanisms of Turbulence* **I**. (Springer-Verlag, 1978), 103-107.

KELLER, J. O., AND DAILY, J. W. 1985, "The Effect of Highly Exothermic Chemical Reaction on a Two-Dimensional Mixing Layer," *AIAA J.* **23**(12), 1937–1945.

KERSTEIN, A. 1988, "A linear-eddy model of turbulent scalar transport and mixing," *Combust. Sci. and Technol.* **60**, 391.

KERSTEIN, A. 1989, "Linear-Eddy Modeling of Turbulent Transport II: Application to Shear Layer Mixing," *Comb. and Flame* **75**, 397–413.

KNIO, O. M. , AND GHONIEM, A. F. 1988, "On the formation of streamwise vorticity in turbulent shear flows," *AIAA* 26$^{\text{th}}$ *Aerospace Sciences Meeting*, AIAA Paper 88-0728.

KOCH, W. 1985, "Local instability characteristics and frequency determination of self-excited wake flows," *J. Sound and Vibration* **99**(1), 53–83.

KOLLMANN, W., AND JANICKA, J. 1982, "The Probability Density Function of a Passive Scalar in Turbulent Shear Flows," *Phys. Fluids* **25**, 1755–1769.

KOLMOGOROV, A. N. 1941, "Local Structure of Turbulence in an Incompressible Viscous Fluid at Very High Reynolds Numbers," *Dokl. Akad. Nauk SSSR* **30**, 299.

KOLMOGOROV, A. N. 1962, "A refinement of previous hypotheses concerning the local structure of turbulence in a viscous incompressible fluid at high Reynolds number," *J. Fluid Mech.* **13**, 82–85.

KONRAD, J. H. 1976, *An Experimental Investigation of Mixing in Two-Dimensional Turbulent Shear Flows with Applications to Diffusion-Limited Chemical Reactions*, Ph.D. thesis, California Institute of Technology.

KOOCHESFAHANI, M. M., AND DIMOTAKIS, P. E. 1986, "Mixing and chemical reactions in a turbulent liquid mixing layer," *J. Fluid Mech.* **170**, 83–112.

KOOCHESFAHANI, M. M., AND DIMOTAKIS, P. E. 1988, "A Cancellation Experiment in a Forced Turbulent Shear Layer," Proceedings, *First National Fluid Dynamics Congress*, 1204–1208.

KOOCHESFAHANI, M. M., DIMOTAKIS, P. E., AND BROADWELL, J. E. 1985, "A 'Flip' Experiment in a Chemically Reacting Turbulent Mixing Layer," *AIAA J.* **23**(8), 1191–1194.

KOOCHESFAHANI, M. M., AND FRIELER, C. E. 1987, "Inviscid Instability Characteristics of Free Shear Layers with non-Uniform Density," *AIAA* 25$^{th}$ *Aerospace Sciences Meeting*, AIAA Paper 87-0047.

KUO, K. K. 1986, *Principles of Combustion* (John Wiley, New York).

LANG, D. B. 1985, *Laser Doppler Velocity and Vorticity Measurements in Turbulent Shear Layers*, Ph.D. thesis, California Institute of Technology.

LASHERAS, J. C., AND CHOI, H. 1988, "Three-dimensional instability of a plane shear layer: an experimental study of the formation and evolution of streamwise vortices," *J. Fluid Mech.* **189**, 53–86.

LELE, S. K. 1989, "Direct Numerical Simulation of Compressible Free Shear Flows," *AIAA* 27$^{th}$ *Aerospace Sciences Meeting*, AIAA Paper 89–0374.

LEONARD, A. 1983, "Numerical simulation of Turbulent Fluid Flows," *Proceedings of the* 3$^{rd}$ *International Symposium on Numerical Methods in Engineering* (edited by P. Lascaux, Pluralis, Paris), 45–63.

LEVENSPIEL, O. 1962, *Chemical Reaction Engineering. An Introduction to the Design of Chemical Reactors.* (John Wiley, New York).

LIEPMANN, H. W., AND ROSHKO, A. 1957, *Elements of Gasdynamics* (John Wiley, New York).

LOWSON, M. V., AND OLLERHEAD, J. B. 1968, "Visualization of noise from cold supersonic jets," *J. Acoust. Soc. Am.* **44**, 624.

MACK, L. M. 1975, "Linear Stability and the Problem of Supersonic Boundary-layer Transition," *AIAA J.* **13**, 278–289.

MARBLE, F. E., AND BROADWELL, J. E. 1977, "The Coherent Flame Model for Turbulent Chemical Reactions," Project SQUID TRW–9–PU.

MASUTANI, S. M., AND BOWMAN, C. T. 1986, "The structure of a chemically reacting plane mixing layer," *J. Fluid Mech.* **172**, 93–126.

MCMURTRY, P. A., JOU, W. H., RILEY, J. W., AND METCALFE, R. W. 1986, "Direct Numerical Simulations of a Reacting Mixing Layer with Chemical Heat Release," *AIAA J.* **24**(6), 962–970.

MCMURTRY, P. A., AND RILEY, J. J. 1987, "Mechanisms by which heat release affects the flow field in a chemically reacting turbulent mixing layer," *AIAA* 25th *Aerospace Sciences Meeting*, AIAA Paper 87–0131.

METCALFE, R. W., ORZAG, S. A., BRACHET, M. E., MENON, S., AND RILEY, J. J. 1987, "Secondary Instability of a Temporally Growing Mixing Layer," *J. Fluid Mech.* **184**, 207–244.

MILLER, P. L. 1991, *Mixing in High Schmidt Number Turbulent Jets*, Ph.D. thesis, California Institute of Technology.

MILLER, P. L., AND DIMOTAKIS, P. E. 1991, "Reynolds number dependence of scalar fluctuations in a high Schmidt number turbulent jet," *Phys. Fluids* A **3**(5), Pt. 2, 1156–1163.

MONIN, A. S., AND YAGLOM, A. M. 1975, *Statistical Fluid Mechanics: Mechanics of Turbulence* II, Ed. J. Lumley (MIT Press, Cambridge, MA).

MUNGAL, M. G., AND DIMOTAKIS, P. E. 1984, "Mixing and combustion with low heat release in a turbulent mixing layer," *J. Fluid Mech.* **148**, 349–382.

MUNGAL, M. G., AND FRIELER, C. E. 1988, "The Effects of Damköhler Number in a Turbulent Shear Layer," *Comb. and Flame* **71**, 23–34.

MUNGAL, M. G, HERMANSON, J. C., AND DIMOTAKIS, P. E. 1985, "Reynolds Number Effects on Mixing and Combustion in a Reacting Shear Layer," *AIAA J.* **23**(9), 1418–1423.

OBOUKHOV, A. M. 1962, "Some specific features of atmospheric turbulence," *J. Fluid Mech.* **13**, 77–81.

OERTEL, H. 1979, "Mach wave radiation of hot supersonic jets investigated by means of the shock tube and new optical techniques," 12th *Int. Symp. on Shock Tubes and Waves*, 266–275.

OSTER, D. , AND WYGNANSKI, I. 1982, "The forced mixing layer between parallel streams," *J. Fluid Mech.* **123**, 91-130.

PAPAMOSCHOU, D. 1988, "Outstanding issues in the area of compressible mixing," *International Workshop on the Physics of Compressible Mixing*, (Proceedings to be published by Springer-Verlag).

PAPAMOSCHOU, D. 1989, "Structure of the compressible turbulent shear layer," *AIAA* 27$^{th}$ *Aerospace Sciences Meeting*, *AIAA J.* **29**(5), 680–681 (1991).

PAPAMOSCHOU, D. , AND ROSHKO, A. 1988, "The Compressible Turbulent Shear Layer: An Experimental Study," *J. Fluid Mech.* **197**, 453–477.

PAREKH, D. E., AND REYNOLDS, W. C. 1989, "Forced Instability Modes in a Round Jet at High Reynolds Numbers," *Phys. Fluids* A **1**(9), 1447.

PITZ, R. W., AND DAILY, J. W. 1983, "Combustion in a Turbulent Mixing Layer at a Rearward-Facing Step," *AIAA J.* **21**(11), 1565–1570.

POPE, S. B. 1981, "A Monte Carlo method for the PDF equations of turbulent reactive flow," *Combust. Sci. and Technol.* **25**, 159-174.

RAGAB, S. A., AND WU, J. L. 1988, "Instabilities in the Free Shear Layer Formed by Two Supersonic Streams," *AIAA* 26$^{th}$ *Aerospace Sciences Meeting*, AIAA Paper 88–0038.

REBOLLO, M. R. 1973, *Analytical and Experimental Investigation of a Turbulent Mixing Layer of Different Gases in a Pressure Gradient*, Ph.D. thesis, California Institute of Technology.

ROBERTS, F. A. 1985, *Effects of a Periodic Disturbance on Structure and Mixing in Turbulent Shear Layers and Wakes*, Ph.D. thesis, California Institute of Technology.

ROBERTS, F. A., AND ROSHKO, A. 1985, "Effects of Periodic Forcing on Mixing in Turbulent Shear Layers and Wakes," *AIAA Shear Flow Control Conference*, Paper 85–0570.

ROGALLO, R. S., AND MOIN, P. 1984, "Numerical Simulation of Turbulent Flows," *Ann. Rev. Fluid Mech.* **16**, 99-137.

ROGERS, M. M., AND MOSER, R. D. 1991, "The three-dimensional evolution of a plane mixing layer. Part 1: The Kelvin-Helmholtz rollup," NASA Technical Memorandum (to appear).

ROTMAN, D. 1991, "Shock wave effects on a turbulent flow," *Phys. Fluids A* **3**(7), 1792–1806.

SABIN, C. M. 1965, "An analytical and experimental investigation of the plane, incompressible, turbulent free-shear layer with arbitrary velocity ratio and pressure gradient," *Transactions of the ASME.* D **87**, 421–428.

SANDHAM, N. D., AND REYNOLDS, W. C. 1987, "Some Inlet-Plane Effects on the Numerically Simulated Spatially-Developing Mixing Layer," 6th *International Symp. on Turb. Shear Flows* (Springer Verlag, 1989), 441–454.

SANDHAM, N., AND REYNOLDS, W. C. 1989a, "The Compressible Mixing Layer: Linear Theory and Direct Simulation," *AIAA* 27th *Aerospace Sciences Meeting*, AIAA–89–0371.

SANDHAM, N. D., AND REYNOLDS, W. C. 1989b, "A Numerical Investigation of the Compressible Mixing Layer," Stanford Report TF–45.

TAM, C. K. W. 1971, "Directional acoustic radiation from a supersonic jet," *J. Fluid Mech.* **46**(4), 757–768.

TAM, C. K. W., AND MORRIS, P. J. 1980, "The radiation of sound by the instability waves of a compressible plane turbulent shear layer," *J. Fluid Mech.* **98**, 349-381.

TAM, C. K. W., AND HU, F. Q. 1988, "Instabilities of supersonic mixing layers inside a rectangular channel," Proceedings, *First National Fluid Dynamics Congress*, 1073–1086.

TOKUMARU, P. T., AND DIMOTAKIS, P. E. 1991, "Rotary Oscillation Control of a Cylinder Wake," *J. Fluid Mech.* **224**, 77–90.

VANDROMME, D., AND HAMINH, H. 1989, "The compressible mixing layer," *Turbulence and Coherent Structures*(Kluwer AP, Dordrecht, 1991), 507–523.

VON NEUMANN, J. 1949, "Recent Theories of Turbulence," in *Collected Works* **VI** (edited by A. H. Taub, McMillan Co., New York, 1963), 437–472.

WAITZ, I. 1991, *An Investigation of Contoured Wall Injectors for Hypervelocity Mixing Augmentation*, Ph.D. thesis, California Institute of Technology.

WALLACE, A. K. 1981, *Experimental Investigation on the Effects of Chemical Heat Release in the Reacting Turbulent Plane Shear Layer*, Ph.D. thesis, U. Adelaide.

WANG, C. 1984, *The effects of curvature on turbulent mixing layers*, Ph.D. thesis, California Institute of Technology.

WEISBROT, I., EINAV. S., AND WYGNANSKI, I. 1982, "The Non Unique Rate of Spread of the Two-Dimensional Mixing Layer," *Phys. Fluids* **25**(10), 1691–1693.

WILLIAMS, F. A. 1988, *Combustion Theory. The Fundamental Theory of Chemically Reacting Flow Systems* ($2^{nd}$ edition, Addison-Wesley, Menlo Park, CA).

WINANT, C. D. , AND BROWAND, F. K. 1974, "Vortex Pairing: The Mechanism of Turbulent Mixing Layer Growth at Moderate Reynolds Number," *J. Fluid Mech.* **63**(2), 237-255.

WYGNANSKI, I. J., AND PETERSEN, R. A. 1987, "Coherent Motion in Excited Free Shear Flows," *AIAA J.* **25**(2), 201–213.

YANG, J. 1991, *An Analytical and Computational Investigation of Shock-Induced Vortical Flows with Applications to Supersonic Combustion*, Ph.D. thesis, California Institute of Technology.

ZHUANG, M., KUBOTA, T., AND DIMOTAKIS, P. E. 1988, "On the Stability of Inviscid, Compressible Free Shear Layers," Proceedings, *First National Fluid Dynamics Congress*, 768–773.

ZHUANG, M., DIMOTAKIS, P. E., AND KUBOTA, T. 1990, "The Effect of Walls on a Spatially Growing Supersonic Shear Layer," *Phys. Fluids* A **2**(4), 599–604.